Dynamic ligand reactivity in a rhodium pincer complex

Tang, Z.; Otten, E.; Reek, J.N.H.; van der Vlugt, J.I.; de Bruin, B.

DOI
10.1002/chem.201501453

Publication date
2015

Document Version
Final published version

Published in
Chemistry - A European Journal

ChemPubSoc Europe

DOI: 10.1002/chem.201501453

CHEMISTRY A European Journal Full Paper

Pincer Complexes |*Hot Paper*|

Dynamic Ligand Reactivity in a Rhodium Pincer Complex

Zhou Tang,[a] Edwin Otten,[b] Joost N. H. Reek,[a] Jarl Ivar van der Vlugt,*[a] and Bas de Bruin*[a]

Dedicated to Professor David Milstein in recognition of his inspirational contributions to the field of cooperative catalysis

Abstract: Ligand cooperativity provides (transition) metal complexes with new reactivities in substrate activation and catalytic reactions, but usually the ligand acts as an internal (Brønsted) base, while the metal acts as a (Lewis) acid. We describe the synthesis and stepwise activation of a new phosphane-pyridine-amide ligand **PNN^{H2}** in combination with Rh^{I}. The ligand is susceptible to stepwise proton and hydride loss from the nitrogen arm (imine formation) and deprotonation at the pyridylphosphine arm (dearomatization), giving rise to amine complex **1**, amido species **2**, imine complex **3** and dearomatized compound **4**. Complex **4** bears a dual-mode cooperative **PNN′** ligand containing both a (nucleophilic) basic methine fragment and a reactive (electrophilic) imine moiety. The basic ligand arm enables substrate deprotonation while the imine ligand arm enables reversible "storage" of the activated (nucleophilic) form of a sulfonamide substrate at the ligand. In combination with metal-based reactivity, this allows for the mono-alkylation of *o*-toluenesulfonamide with iodomethane. Compounds **1**, **3** and **4** are structurally characterized. We also report the first structurally characterized example of an aminal in the coordination sphere of rhodium, complex **5**, [Rh(CO)(**PNN″**)], formed by sequential N–H activation of sulfonamide by the dearomatized ligand **PNN′** and follow-up nucleophilic attack of anionic sulfonamide onto the imine fragment.

Introduction

Pincer-type transition-metal complexes have been extensively studied and applied in a wide range of bond activation and catalytic reactions, due to their high stability and synthetic versatility.[1] Recently, the introduction of metal–ligand bifunctional substrate activation[2] has further boosted applications of pincer metal complexes and have opened up new opportunities for catalyst design. Cooperative ligands assist the metal center in bond-breaking and bond-making processes by directly participating in substrate activation or product formation.[2a] This cooperative effect provides the metal complexes with new reactivities to promote reactions using more environment-benign reagents and conditions[3] and also provides opportunities to replace noble metals with more abundant base metals.[4] Various ligand designs, both pincers and otherwise, have proven efficient for metal–ligand bifunctional substrate activation and cooperative catalysis.[5] Among them, proton-responsive donor-appended picolyl- and lutidyl-based systems have attracted much attention due to the broad substrate scope.[6–8] A common feature of most reported cooperative ligand concepts is the function of an internal (Brønsted) base, which reversibly accepts protons from substrates, while the metal functions as a (Lewis) acid.

Examples of metal-ligand cooperativity that extends beyond substrate activation via a Lewis acidic metal and Brønsted basic ligand site are rare. Most of those are limited to substrate activation by simultaneous binding of the substrate to a vacant (transition) metal site and to a hydrogen-bond donor or acceptor,[9] with a borane ligand as a hydride mediator,[10] or radical-type activation with transition metal complexes bearing redox-active ligands.[11] To the best of our knowledge, using a reactive Schiff-base functionality in the ligand framework to reversibly "store" an activated substrate in the periphery of the active (transition) metal site in order to enable subsequent coupling with another substrate is thus far not reported using cooperative catalysis.[12] This approach of cooperative substrate activation is demonstrated for the selective mono-methylation of sulfonamides using a Rh^{I}(**PNN**) system (Figure 1), designed to encompass both nucleophilic and electrophilic reactivity in the ligand framework. We describe a series of stoichiometric reactions that form a hypothetical catalytic cycle when combined. Some unwanted side-reactions prevent true catalytic turnover in one-pot reactions, but the described approach may be able to accelerate other catalytic reactions.

We argued that ligands that contain both a Brønsted basic site and an imine functionality might enable new modes of cooperative substrate activation processes. Therefore, a new PNN ligand platform that offers several reactive sites was designed.

[a] *Z. Tang, Prof. Dr. J. N. H. Reek, Dr. Ir. J. I. van der Vlugt, Prof. Dr. B. de Bruin*
Homogeneous, Bio-inspired & Supramolecular Catalysis
van 't Hoff Institute for Molecular Sciences, University of Amsterdam
Science Park 904 (The Netherlands)
E-mail: j.i.vandervlugt@uva.nl
b.debruin@uva.nl

[b] *Dr. E. Otten*
Stratingh' Institute, University of Groningen
Nijenborgh 8, Groningen (The Netherlands)

Supporting information for this article is available on the WWW under http://dx.doi.org/10.1002/chem.201501453.

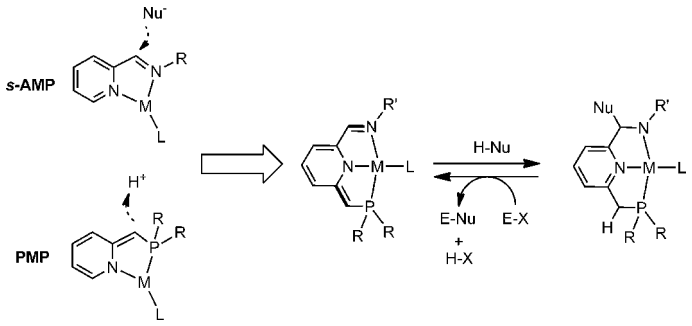

Figure 1. Concept of sequential proton-nucleophile reactivity combined within one dual-mode reactive pincer scaffold.

It is known that *sec*-aminomethylpyridine ligands (*s*-AMP), when bound in their amido form to a transition metal, have a tendency to lose a hydride (or the overall equivalent of one proton and two electrons) from the methylene group, resulting in oxidation to the imine form,[13,14] which is then electrophilic and thus susceptible to coupling with a nucleophile. This feature could provide an opportunity for ligand-assisted sequential proton and nucleophile transfer chemistry when combined with PMP-derived dearomatization reactivity (PMP = phosphinomethylpyridine; Figure 1). We herein describe the coordination chemistry of such a hybrid PNN-ligand to Rh^{I} and demonstrate the multiple activation and monoalkylation of a primary sulfonamide as a test-case for this new concept.

Results and Discussion

Synthesis of amine-complex 1, [Rh(CO)(PNN^{H3})]PF$_6$

PNN ligand **PNN^{H3}** was prepared using a modified literature procedure (Scheme 1),[15] involving sequential phosphorylation and amination of 2,6-bis(chloromethyl)pyridine with di-*tert*-butylphosphine borane and 2,6-diisopropylaniline, respectively. The product ligand **PNN^{H3}** was obtained as a white solid in an overall yield of 43% by refluxing a diethylamine solution of the resulting product **PNN^{H3}·BH$_3$**, followed by facile work-up.

The reaction of two equivalents of ligand **PNN^{H3}** (in MeOH) with $[Rh(CO)_2(\mu\text{-}Cl)]_2$ (in MeOH) resulted in immediate formation of a brownish-yellow solution. Addition of KPF_6 or NH_4PF_6 followed by partial evaporation and filtration afforded the cationic carbonyl complex [Rh(CO)(**PNN^{H3}**]PF_6 (**1**) (Scheme 2). The complex exhibits a sharp doublet at 96.4 ppm ($J_{Rh\text{-}P}$ 155.8 Hz) in the ^{31}P NMR spectrum. The signals for the two isopropyl C–H protons appear as broad multiplets at 4.50 and 3.24 ppm in the ^{1}H NMR spectrum, indicating a stable coordination mode of the pyramidal tertiary amine donor to rhodium and hindered rotation of the diisopropylphenyl group around the C–N bond.

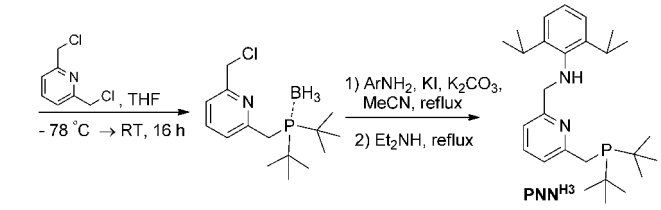

Scheme 1. Synthetic route to ligand **PNN^{H3}**.

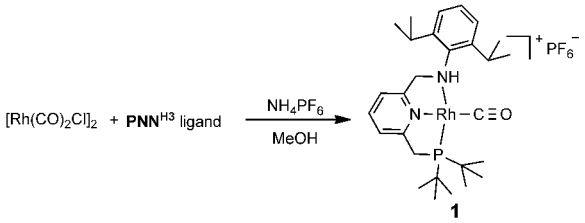

Scheme 2. Synthesis of amine complex **1**.

Synthesis of the amido derivative 2, [Rh(CO)(PNN^{H2})]PF$_6$, imine-complex 3, [Rh(CO)(PNN^{H})]$^+$ and its dearomatized derivative 4, Rh(CO)(PNN′)

Addition of one equivalent of potassium *tert*-butoxide (KO*t*Bu) to a C_6D_6 suspension of **1** led to a doublet at 88.1 ppm ($\Delta\delta = -8.3$) in the ^{31}P NMR spectrum, with a remarkably smaller $J_{Rh\text{-}P}$ of 129.7 Hz ($\Delta J = -26.1$) compared to that of complex **1**, in agreement with the presence of a stronger donor *trans* to P.[16] The ^{1}H NMR spectrum showed no -N*H* signal, which supports formulation of this complex as the neutral amido complex Rh(CO)(**PNN^{H2}**) (**2**) (Scheme 2). Complex **2** is not stable at room temperature, and transforms into other species, see below. Stirring a mixture of in situ formed amido-complex **2** (generated by deprotonation of **1** using 1 equiv KO*t*Bu) and sodium bicarbonate ($NaHCO_3$) in THF overnight led to unexpected formation of a major brown product (**3**) and a minor dark blue product (**4**) after work-up (Scheme 3).

The brown species shows a doublet (96.3 ppm ($\Delta\delta$ 0.1); $J_{Rh\text{-}P}$ 149.3 Hz ($\Delta J = -6.5$)) in the ^{31}P NMR spectrum and a doublet of doublets at 8.39 ppm (C*H*=N) in the ^{1}H NMR spectrum, which correlates with a peak at 168.87 ppm in the ^{13}C NMR spectrum according to 2D ^{1}H–^{31}C HSQC spectroscopy. These data indicated formation of the imine complex **3**, [Rh(CO)(**PNN^{H}**)]$^+$. One possible pathway involves deprotonation of complex **1** by KO*t*Bu to form amido complex **2**, followed by hydride transfer from the amidomethylene arm of **2** to the proton of $NaHCO_3$. In the presence of KPF_6 (generated in the first deprotonation step of **1** with KO*t*Bu) this would yield the PF_6 salt of imine complex **3**, with H_2 and insoluble $KNaCO_3$ as side products. An alternative, albeit very similar mechanism leading to formation of complex **3** involves spontaneous loss of H_2 from complex **2** to form complex **4** (see below), followed by protonation of **4** to produce complex **3** (see Scheme 3). In this case, amphoteric $NaHCO_3$ (possibly combined with some adventitious water) would act as the proton donor in the last step (**4** + KPF_6 + $NaHCO_3$ → **3** +

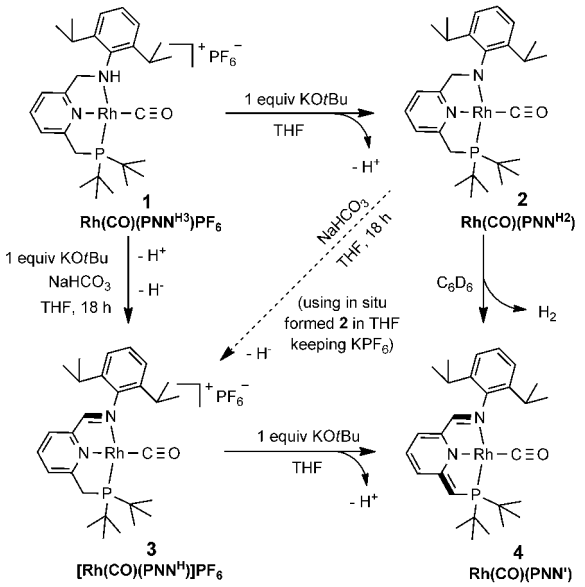

Scheme 3. Formation of imine ligand complex **3** from amido complex **2** with $NaHCO_3$ and subsequent deprotonation to give dearomatized complex **4** in THF and spontaneous H_2 loss from **2** to form **4** in benzene.

$KNaCO_3$). In agreement with both possible mechanisms, H_2 was detected by GC taking a sample from the headspace after reaction. An unidentified intermediate species in the reaction of **2** to **3** or **4** in the reaction with $NaHCO_3$ in THF is detectable by NMR spectroscopy (see Supporting Information Figure S3, S4), but this species was not isolated or further characterized. When ^{13}C-labeled $NaH^{13}CO_3$ was used, no formate was detected using ^{13}C NMR spectroscopy, thus excluding carbonate as a hydride acceptor.[17]

Addition of a second equivalent of KO*t*Bu to imine species **3** in THF instantaneously led to a drastic color change from brown to dark-blue. The ^{31}P NMR spectrum indicated complete conversion to a single species, exhibiting a doublet at 89.2 ppm (J_{Rh-P} = 156.3 Hz), while the pyridine protons are shifted markedly upfield (5.37–6.35 ppm) in the corresponding ^{1}H NMR spectrum, thus pointing to "dearomatization". The CO stretch of **4** appears at 1950 cm^{-1} in the IR spectrum ($\Delta\nu$ = −46 cm^{-1} compared to **1**). These observations are consistent with formulation of this complex as the dearomatized imine complex **4**, Rh(CO)(**PNN**′), featuring a formal amido nitrogen *trans* to CO. The imine C–H appears as a doublet of doublets at 7.01 ppm, with long-range couplings to rhodium ($^3J_{Rh-H}$ 2.8 Hz) and phosphorus ($^4J_{P-H}$ = 4.6 Hz). The doublet at 5.34 ppm ($^2J_{P-H}$ = 2.9 Hz) is assigned to the methine proton (C=C*H*-P).

Interestingly, complex **4** was also obtained by simply storing a C_6D_6 solution of the amido complex **2** at room temperature, while dihydrogen (H_2) was detected as a byproduct both with ^{1}H NMR spectroscopy (solution phase) and gas chromatography (GC) (head-space above the solution) (Supporting Information, Figures S1, S2, S27). This reaction involves formal loss of a hydride from the amido methylene arm and a proton from the phosphane methylene arm of the same ligand to generate H_2 through either a concerted inter- or intramolecular process. The spontaneous loss of H_2 is unusual and this observation nicely demonstrates the complementary reactivity of the two arms and the synergy between these electronically distinct moieties. Complex **4** could also be synthesized simply by stirring a CH_2Cl_2 solution of **1** overnight in the presence of excess sodium hydroxide (NaOH).

The corresponding X-ray structures for **3** and **4** are depicted in Figure 2, together with the structure of complex **1**. Yellow single crystals for complex **1** were obtained by slow diffusion of pentane into a concentrated solution of **1** in dichloromethane. Brownish-red colored crystals of **3** were obtained from slow diffusion of diethyl ether into a concentrated solution of **3** in dichloromethane. X-ray structure determination provided the structures depicted in Figure 2. Both complexes adopt a nearly perfect square planar geometry around Rh, with the plane defined by the atoms P_1, N_1 and N_2. The N2–C1 bond in **3** is markedly shorter than in **1** (1.496(4) Å in **1** vs. 1.284(3) Å in **3**), indicating genuine imine double bond character in **3**. Dark-colored single crystals of **4** were obtained from a concentrated pentane solution of **4** at −78 °C. The square planar geometry around rhodium is maintained in the conversion of **3** to **4**. The short C_6–C_7 and C_1–N_2 bond lengths indicate double bond character for these bonds in **4**.

The short Rh_1–N_1 bond length of 2.0264(14) Å and the alternating C–C bond lengths in the heterocycle (not shown) are consistent with dearomatization of the pyridine fragment. The Rh_1–N_2 and Rh_1–P_1 bond lengths vary only marginally between the cationic amine and imine species and the dearomatized neutral imine derivative. The N_2-Rh_1-P_1 and N_2-Rh_1-P_1 angles also do not differ substantially, showing the structural integrity of the overall tridentate scaffold upon multiple proton-transfer

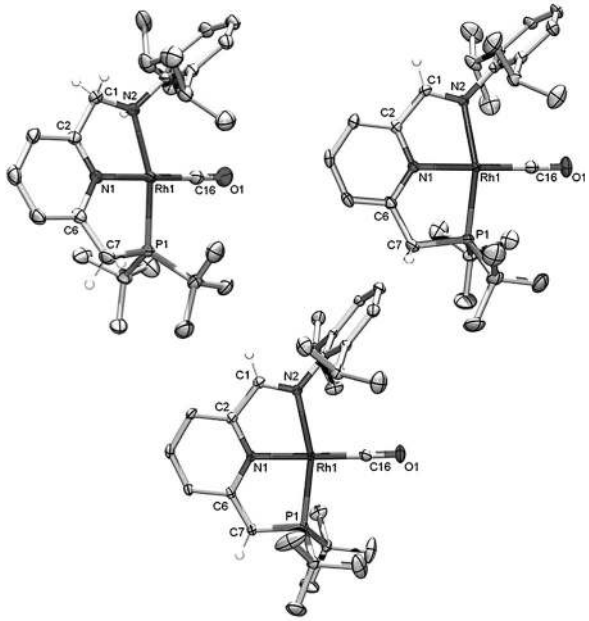

Figure 2. ORTEP plots (50% probability ellipsoids) of cationic amine complex **1**, imine complex **3** and dearomatized neutral derivative **4**. Disorder, counter-ions, lattice solvent and hydrogen atoms are omitted for clarity, except for those located on C_1 and C_7.

Table 1. Selected bond lengths [Å] and angles [°] for complexes **1**, **3** and **4**.

	1	3	4
Rh_1–N_1	2.057(2)	2.0427(18)	2.0264(14)
Rh_1–N_2	2.156(3)	2.0885(19)	2.1191(14)
Rh_1–P_1	2.2337(8)	2.2395(7)	2.2641(5)
Rh_1–C_{16}	1.829(3)	1.829(3)	1.8198(19)
N_2–C_1	1.496(4)	1.284(3)	1.389(2)
C_6–C_7	1.496(4)	1.498(4)	1.367(2)
C_{28}–O_1	1.143(3)	1.151(3)	1.157(2)
P_1-Rh_1-N_1	84.64(7)	83.96(6)	82.89(4)
P_1-Rh_1-N_2	162.84(7)	161.55(5)	160.46(4)
Rh_1-N_2-C_1	111.42(18)	115.13(15)	113.65(12)
Rh_1-P_1-C_7	100.62(10)	101.11(8)	100.84(6)
N_1-Rh_1-C_{28}	179.11(13)	179.26(10)	178.90(7)
Rh_1-C_{28}-O_1	178.8(3)	178.8(2)	178.36(16)

reaction steps. The methylene groups are located above and below the Rh-P-N-N plane in **1**, whereas complexes **3** and **4** display a virtually flat extended structure, indicative of significant π-conjugation. Selected bond lengths and angles for the three complexes are compared in Table 1.

To obtain further insight in the electronic structure of the dearomatized imine-ligand complex **4**, we switched to DFT calculations (BP86/def2-TZVP) (Figure 3). The highest occupied molecular orbital (HOMO) is found to reside predominantly on the electron-rich methine carbon of the phosphine arm, in accord with calculations on other dearomatized pincer complexes,[6,8,18,19] with a minor contribution from the dearomatized pyridine. The corresponding lowest unoccupied molecular orbital (LUMO) is also found to be predominantly ligand-based, residing mainly on the electron-deficient imine fragment. The combination of both a ligand-based HOMO, relevant for reactivity toward electrophiles, and a ligand-based LUMO (susceptible for attack by nucleophiles) is highly unusual, and shows that the complex is likely to display ligand-based reactivity in reactions with both electrophilic and nucleophilic substrates. The LUMO of **3** is also localized mainly at the imine fragment, with a similar shape as that of **4**, which means the imine functionality of **4** is maintained for nucleophilic addition after the first electrophilic addition (e.g. protonation of the methine). The reactivity of such "Janus-like" ligands is ill-explored but potentially interesting in the context of cascade catalysis.

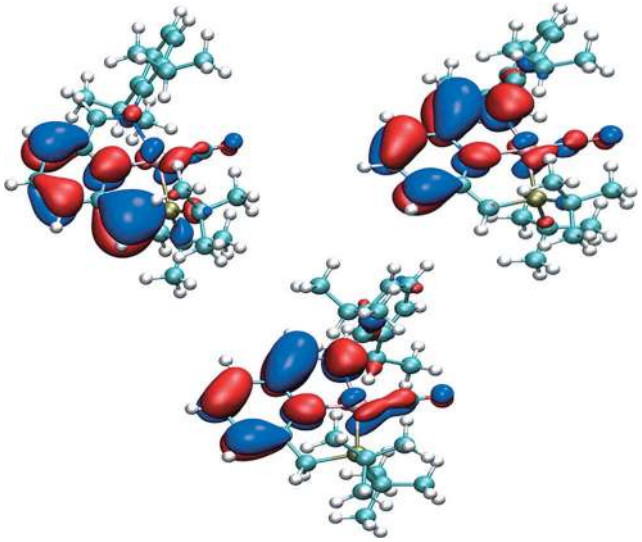

Figure 3. DFT calculated (BP86/def2-TZVP) frontier orbitals for imine-complex **4** (dearomatized) and **3** (aromatized) (top left: HOMO of **4**; top right: LUMO of **4**; bottom: LUMO of **3**).

Reactivity of 4 towards a weakly nucleophilic amine base

Complex **4** was found to be inert toward H_2, benzyl alcohol or aniline under mild conditions, which is attributed to the rigid nature of the ligand backbone, in particular the imine fragment. It seems that the extended conjugated π-system of the **PNN′**$^-$ ligand in **4** does not have the required flexibility to accommodate a favorable transition state for proton transfer from a metal bound substrate to the electron-rich methine arm. Reprotonation of the phosphine arm (the HOMO) with stronger protic acids such as HCl, formic acid or benzoic acid is feasible, generating derivatives of **3**. However, in case of formic acid as substrate for example, further reaction involving hydride transfer from a metal-bound or outer-sphere formate to the imine fragment (the LUMO) to generate an analogue of **2** was not observed. This indicates that the corresponding amido-form of the ligand (**PNN′**$^{H2-}$) is thermodynamically unstable with respect to the neutral imine-ligand form (**PNN′**).[13]

Interestingly and in stark contrast with the other substrates tested, complex **4** reacted almost instantaneously with one molar equivalent of *o*-toluenesulfonamide (***o*TsNH$_2$**) in CD_2Cl_2, as indicated by a color change from deep-blue to light-yellow (Scheme 4). Spectroscopic data showed that the reaction involved both reactive ligand arms of the complex, leading to both protonation of the electron-rich methine arm attached to the P-donor and nucleophilic attack of the deprotonated sulfonamide to the electrophilic imine functionality.[20] This reactivity is quite remarkable, as sulfonamides are poorly nucleophilic[21] and thus should not be able to attack the imine functionality of **4** in a direct "outher-sphere" mechanism. The IR spectrum showed a CO stretch at 1983 cm^{-1}, suggestive of rearomatization of the pyridine ring. Notably, the ^{31}P NMR spectrum showed clean conversion to a single species, represented by a doublet at 94.2 ppm with a coupling constant $J_{Rh\text{-}P}$ of 149.3 Hz. Likewise, ^{1}H NMR and ^{13}C NMR spectroscopy revealed clean conversion of **4** to **5** (see Experimental Section and Supporting Information). HR-MS spectrometry (*m/z* 724.2250 for [*M*−H$^+$]) indicates the incorporation of the sulfonamide substrate as well as preservation of the original diisopropylanilidyl fragment. These combined data support formulation of this species as the neutral aminal complex **5** (Scheme 4).

An unexpected rearrangement of the donor atoms has occurred to generate this addition product, with the sulfonamido nitrogen donor coordinated to Rh, while the original imine-donor is transformed into a non-coordinated aniline moiety. The aniline NH moiety resonates at 3.75 ppm in the ^{1}H NMR spectrum, and gives rise to a sharp doublet ($^3J_{HH}$ = 10.3 Hz). The relatively large $^3J_{HH}$ coupling constant corresponds to an

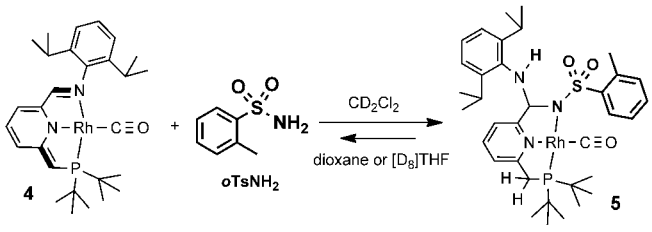

Scheme 4. Reversible reaction of *o*-toluenesulfonamide with complex **4** to generate aminal complex **5** [Rh(CO)(**PNN**′)].

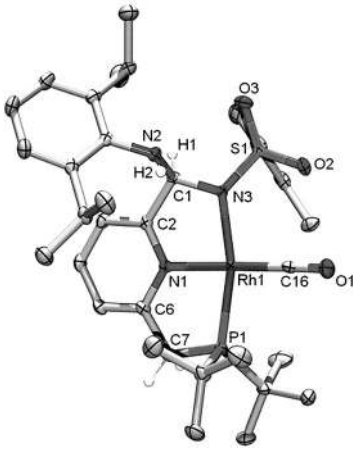

Figure 4. ORTEP plot (50% probability ellipsoids) of aminal complex **5**. Lattice solvent (CH_2Cl_2) and hydrogen atoms removed for clarity, except for H_1 and H_2, belonging to the aminal fragment. Selected bond lengths [Å] and angles [°]: Rh_1–N_1 2.057(2), Rh_1–N_3 2.083(2), Rh_1–P_1 2.2251(8), Rh_1–C_{16} 1.821(3), P_1–C_7 1.857(3), C_6–C_7 1.499(4), N_3–C_1 1.460(3), N_2–C_1 1.482(3), C_1–C_2 1.520(3), Rh_1–C_{16} 1.155(4), C_{16}–O_1 1.155(4); N_3-Rh_1-P_1 162.93(6), P_1-Rh_1-N_1 84.43(6), N_1-Rh_1-C_{16} 176.37(10), Rh_1-C_{16}-O_1 177.7(2), Rh_1-N_3-C_1 114.28(15), Rh_1-P_1-C_7 100.85(10).

antiperiplanar configuration of the N–H and the tertiary PyC–H protons, in agreement with the X-ray structure. Amines typically give rise to broad featureless signals as a result of rapid exchange with other amines or for example, water. The fact that the aniline NH moiety is present as a sharp doublet suggests that it is in a rigid configuration and does not undergo rapid proton exchange with exogenous proton donors (e.g., water). Initially we took this as an indication for H-bonding between the NH moiety and one of the sulfonyl oxygen atoms, but spectroscopic investigations are inconclusive about the existence of such an H-bond. NMR spectroscopy did confirm that the NH moiety adopts a preferred configuration in solution. Detailed analysis of the ^{1}H, ^{1}H-COSY, ^{1}H-NOESY, and ^{1}H^{13}C-HSQC spectra of the complex showed that the N–*H* moiety has stronger NOE contacts with only one of the two isopropyl moieties. The structure of **5**, [Rh(CO)(**PNN**′)], was further corroborated by X-ray structure determination of single crystals grown from dichloromethane and diethyl ether. The X-ray structure (Figure 4) indeed shows a highly congested aminal in the coordination sphere of a square planar Rh$^{\text{I}}$ center, but no hydrogen-bond interaction is observed between the N–*H* moiety and the sulfonyl oxygen atoms. The N–*H* and the tertiary PyC–*H* hydrogen atoms are oriented in an antiperiplanar configuration, with the NH moiety pointing toward one of the isopropyl groups, in accordance with the NMR data. Apparently the conformation of the NH moiety observed in the solid state is also the preferred orientation in solution, and in contrast to our initial assumptions this might not be caused by H-bonding but seems rather a result of the steric congestion around the N–*H* moiety (as revealed by the X-ray structure), thus leading to slow proton exchange at the amine nitrogen atom on the NMR time scale. To the best of our knowledge, this is the first report of a structurally characterized aminal in the coordination sphere of rhodium. Furthermore, this reaction constitutes the breaking of two N–H bonds and the formation of one C–H, one C–N and a novel N–H bond.

The reaction likely proceeds via initial proton transfer from the activated sulfonamide to the nucleophilic methine of the phosphine arm, resulting in rearomatization of the pyridine ring. This may occur in either an outer-sphere manner (bimolecular process) or via pre-coordination of the sulfonamide to Rh (unimolecular process). The resulting (rhodium) sulfonamido intermediate can then undergo addition to the electrophilic imine carbon, with a subsequent 1,3-proton shift to generate the observed aminal. The latter (intermolecular) process involving pre-coordination of the sulfonamide process seems most likely.

In dynamic combinatorial chemistry,[22] imine formation is often reversible in the presence of water. In analogy, aminal **5** is highly sensitive to the type of solvent used. Upon switching from CD_2Cl_2 to dioxane or [D_8]THF (Scheme 4) and under mild heating, complex **5** reverts to **4**, as monitored by ^{31}P NMR spectroscopy. In addition, HR-MS spectra of complex **5** measured in positive ion mode showed only *m/z* 555.2033, corresponding to complex **4** plus a proton (calcd *m/z* 555.2006) (Supporting Information, Figures S5–S7). The conversion of **5** to **4** in THF and dioxane is most likely a result of the different solubility of **5** (poorly soluble) and the mixture of **4** and *o*TsNH$_2$ (well soluble) in these solvents. Adventitious H_2O might also play a role. Note that organic aminals are typically unstable with respect to their precursors, and hence isolation of complex **5** is highly unusual.

The reversible making and breaking of the aminal C–N bond under mild conditions suggests that this complex has potential in productive C–N bond functionalization protocols, using the cooperative ligand system in concert with metal-based activity. Hence, as proof-of-concept, the coupling of sulfonamides with iodomethane (MeI) was investigated (Scheme 5). Selective mono-alkylation of sulfonamides (and amines in general) under mild conditions, minimizing the generation of undesirable waste, is still a challenging task in organic synthesis.[23] Heating an equimolar mixture of MeI and **5** in CD_2Cl_2 at 60 °C for 30 min resulted in the formation of complex **3**′, an analogue of complex **3** but with iodine as the counter-ion, and the *N*-methylsulfonamide product (*N*,2-dimethylbenzene sulfonamide, ***o*TsNHMe**) in 21 and 11% yield, respectively (according to ^{1}H NMR spectroscopy). Continued heating for 22 h increased the yield of these two species to 79% and 51%, respectively, based on ^{1}H NMR integration (Supporting Informa-

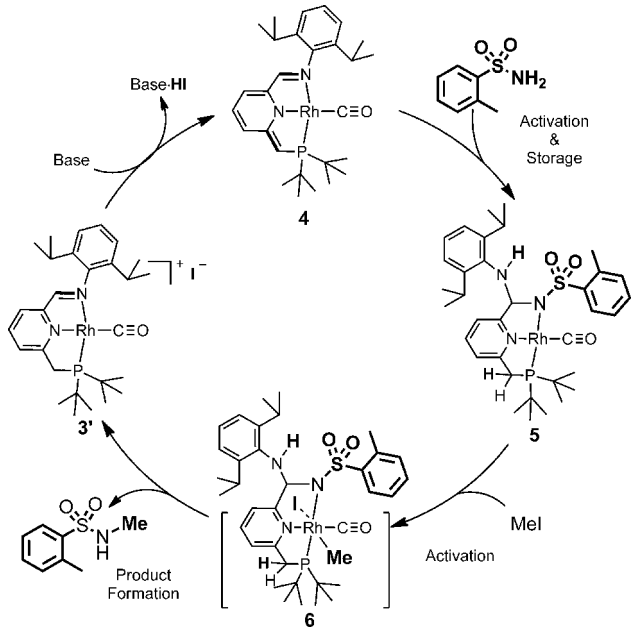

Scheme 5. Hypothetical cycle composed of stoichiometric steps (one turnover) involving mono-methylation of ***o*-TsNH$_2$** with MeI mediated by **4**.

tion, Scheme S2, S3, Figure S8–S12). The formation of complex **3′** and ***o*TsNHMe** was confirmed by independent synthesis of the two species and comparing the NMR spectra. The organic ***o*TsNHMe** product is presumably generated by consecutive oxidative addition of MeI, forming intermediate **6**, and reductive C–N bond formation at Rh^{I} (see Scheme 5). Addition of base (KO*t*Bu) regenerates the dearomatized complex **4**, which should be susceptible to renewed attack by sulfonamide and thereby close the hypothetical catalytic cycle (Scheme 5). This sequence is composed of the following steps: 1) ligand-aided splitting of the N–H bond of sulfonamide by **4**, with the electrophilic and the nucleophilic part residing on the P and N arm of the ligand, respectively. 2) Oxidative addition of MeI to generate a Rh^{III} complex (either five- or six-coordinated). 3) Reductive C–N bond formation to generate imine-complex **3′** and the *N*-methylated sulfonamide product. 4) Deprotonation of complex **3′** to regenerate the starting complex **4**.

As such, the combined reactions closes a catalytic cycle for mono-alkylation of sulfonamides with MeI, which proceeds via the discrete and well characterized intermediates **3′**, **4** and **5**. Attempts to detect the proposed Rh^{III} intermediate **6** by in situ ^{31}P NMR spectroscopy were not successful, and only complexes **5** and **3′** were observed. This is probably due to the transient nature of **6** on the NMR time-scale due to rapid reductive elimination of ***o*TsNHMe** to yield complex **3′**. Direct coupling of MeI with the sulfonamide nitrogen with the sulfonamide without forming a Rh^{III} intermediate cannot be completely excluded, but seems unlikely. Any direct coupling would be expected to occur on the aniline nitrogen of the aminal, which should be more nucleophilic than the sulfonamide nitrogen (which is involved in delocalization to the sulfonyl moiety). No reaction was observed between ***o*TsNH$_2$** and MeI in the absence of complex **5** under the same conditions, or in the presence of Na_2CO_3, thus showing that the reaction is mediated by the Rh complex. This sequence represents, to our best knowledge, the first example of such unique new metal–ligand cooperativity for productive substrate functionalization, although some recent cooperative substrate functionalisation strategies and reversible directing group strategies bear some similarities with this concept.[12b,c,24] We anticipate that the reaction sequence shown in Scheme 5 can be extended to other "electrophile-nucleophile" combinations, and further (catalytic) coupling reactions with additional substrates might be realized based on this dual-mode ligand cooperativity.

Elucidation of side-reactions

The reaction shown in Scheme 5 is composed of individual stoichiometric steps. A catalytic reaction involving multiple turnovers is prevented by competing side reactions. To shed more light on the catalyst deactivation pathways, we decided to explore the formation of side products (in particular deactivated rhodium complexes) under (pseudo-) catalytic conditions. Quite remarkably, and contrary to previous observations on the reactivity of carbon electrophiles with dearomatized pincer ligands,[18,25] the addition of MeI to **4** did not result in ligand-based C–C coupling at the methine moiety adjacent to the phosphine donor. The inertness of the **PNN′**$^{-}$ fragment is attributed to the electron-withdrawing effect of the imine moiety, which decreases the overall nucleophilicity of the ligand framework (decrease of the HOMO relative to, for example, a dearomatized PNP ligand). MeI also does not oxidatively add to the Rh^{I} center of **4**, which may be explained by a stabilizing push–pull effect (π-donation from the dearomatized pyridine nitrogen lone pair to a Rh d orbital (push) is balanced by π-back donation from Rh to the π^* orbital at CO (pull)). Addition of *N*-methyl-phenylsulfonamide to **4** under the same conditions as for the coupling reaction of **5** and MeI did not result in any addition product. Therefore, neither MeI nor the monoalkylated sulfonamide product interfere with the envisioned catalyst. Hence, neither product inhibition nor inhibition by unwanted reactions with the MeI substrate seems to cause any problems in the envisioned catalytic reaction. However, the aminal fragment in complex **5** appears susceptible to hydrolysis in wet solvent over the course of several days. Under these conditions, release of free aniline was detected, and NMR spectroscopy further pointed to formation of complex **8**, which results from attack of hydroxide to the imine moiety of the proposed imine intermediate **7**, which is formed after expulsion of aniline (Scheme 6).

The -CH(O*H*) proton appears as a sharp doublet at 4.30 ppm ($^{3}J_{H\text{-}H}$ = 2.5 Hz), while the -C*H*(OH) proton shows up at 6.12 ppm as a doublet-of doublet ($^{3}J_{H\text{-}H}$ = 2.4 Hz, $^{4}J_{P\text{-}H}$ = 2.0 Hz), when measured in CD_2Cl_2. Upon addition of [D$_4$]MeOH, the -OH signal disappeared. Besides **8**, also another side-product, **9** was detected that potentially hinders catalytic turnover. Like **8**, this species also seems to be derived from intermediate **7** (again formed by aniline elimination from the aminal moiety of **5**). Complex **9** is formed more rapidly in the presence of an excess sulfonamide, and bears two sulfonamide fragments

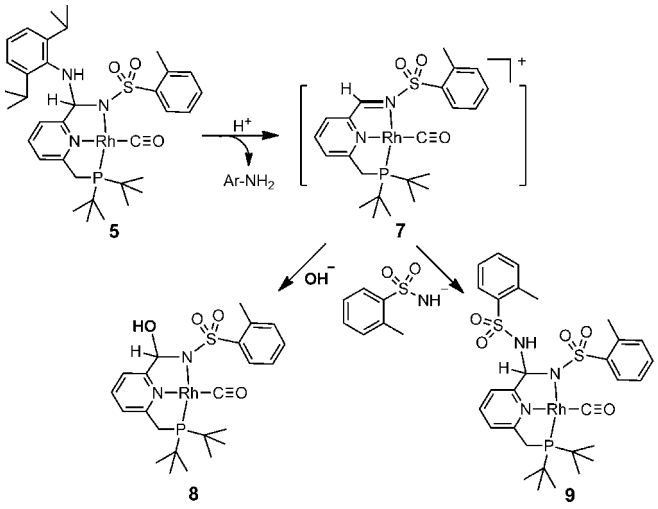

Scheme 6. Transformation of complex **5** into **8** and **9**, upon reaction with water and excess sulfonamide, respectively.

(Scheme 6). Hence, complex **9** was also identified as the major "resting state" (±80%) in a (pseudo) catalytic test-reaction using five molar equivalents of the sulfonamide substrate. Interestingly, *m/z* values corresponding to complex **7**[M^+] as the major peaks were always observed in the ESI-MS spectra of **8** or **9** in positive ion mode (Supporting Information, Figures S71–S72), while **8** or **9** were not detected. This may suggest reversible sulfonamide addition to the imine arm of the ligand of **7**. The reactive sulfonimine carbon of the proposed intermediate **7** is likely more susceptible to nucleophilic attack than the aniline-based imine carbon of **3**, which is stable in aqueous conditions. The most likely pathways for conversion of complex **5** into **8** and **9** are shown in Scheme 6, but alternative mechanisms cannot be excluded.

Finally, the requirement of a strong base like tBuO$^-$ to deprotonate **3** and thus regenerate **4** imposes limitations on the development of catalytic reactions, as these nucleophilic bases react with the MeI substrate.

Conclusion

We have reported the synthesis of a unique (phosphane)(amine)pyridine ligand **PNN^{H3}** and its versatile coordination chemistry with Rh^{I}. This includes selective, stepwise transformations from the neutral **PNN^{H3}** amine ligand in complex **1**, to the anionic **PNN^{H2-}** amido ligand in complex **2**, the neutral **PNN$^{H'}$** imine ligand in complex **3** and the anionic "dearomatized" imine ligand **PNN$^{H'-}$** in complex **4**. The ligand is capable of selective dual-mode reactivity and is susceptible to both electrophilic and nucleophilic attack. The X-ray structures of **1**, **3**, and **4** show subtle but significant differences between these species. DFT calculations show that both the HOMO and LUMO of **4** are ligand-based, which is rather unique. This complex readily activates both N–H bonds of *o*-toluenesulfonamide in dichloromethane, resulting in selective C–N bond formation to generate the unique aminal complex **5**, which was also structurally characterized. The addition reaction is found to be reversible by switching to a more polar solvent. MeI is successfully used as an electrophile to couple with the activated sulfonamide, selectively generating the *N*-methylsulfonamide. This proof-of-concept coupling reaction demonstrates the viability of a new type of metal-ligand cooperativity mechanism involving two electronically distinctly different ligand arms to activate both N–H bonds of the sulfonamide substrate. Although the overall reaction is inhibited when using an excess of the substrate due to the occurrence of side-reactions, dual-mode ligand reactivity in general may be a viable approach for catalysis.

Experimental Section

General methods: All reactions were carried out under an argon atmosphere using standard Schlenk techniques or in a glovebox unless noted otherwise. With exception of the compounds given below, all reagents were purchased from commercial suppliers and used without further purification. 2-(Chloromethyl)-6-((di-*tert*-butylphosphino)-methyl)pyridine·BH_3 was synthesized according to a reported procedure.[15] Sodium (*o*-tolylsulfonyl)amide was synthesized by reacting 2-methylbenzenesulfonamide with stoichoimechic sodium methoxide in methanol solution. THF, dioxane, pentane, and diethyl ether were distilled from sodium benzophenone ketyl under nitrogen. CH_2Cl_2, and methanol were distilled from CaH_2 under nitrogen. NMR spectra (^{1}H, ^{31}P{^{1}H} and ^{13}C{^{1}H}) were measured on a Bruker AMX 400 spectrometer at 25 °C unless noted otherwise. IR spectra were recorded with a Nicolet Nexus FT-IR spectrometer. HR-MS were obtained using a time-of-flight JEOL AccuTOF LC-plus mass spectrometer (JMS-T100 LP).

Ligand PNN^{H3}·BH_3: An acetonitrile solution (50 mL) of 2-(chloromethyl)-6-((di-*tert*-butylphosphino)methyl)pyridine·BH_3 (500.0 mg, 1.669 mmol, 1 equiv), 2, 6-diisopropylaniline (0.330 mL, 1.752 mmol, 1.05 equiv), potassium iodide (27.7 mg, 0.167 mmol, 0.1 equiv) and potassium carbonate (1153 mg, 8.345 mmol, 5.0 equiv) was refluxed for 20 h. All volatiles were removed under vacuum, dichoromethane (30 mL) was added and the solution was washed with brine and dried with sodium sulfate. The pure product was obtained after silica column chromatography (hexane/ethyl acetate) as a white solid (345.4 mg, 47%). ^{1}H NMR (400 MHz, CD_2Cl_2): δ = 7.60 (t, J = 7.7 Hz, 1H$_{py4}$), 7.51 (d, J = 7.7 Hz, 1H$_{Py}$), 7.16–7.06 (m, 1H$_{Py}$ + 3H$_{Ar}$), 4.11–4.10 (br m, 2H$_{Py\text{-}CH2N}$ + 1H$_{NH}$), 3.43–3.36 (m, 2H$_{Ph\text{-}C(CH3)2H}$ + 2H$_{Py\text{-}CH2P}$), 1.30 (d, J = 12.6 Hz,18H$_{C(CH3)3'}$), 1.25 (d, J = 6.9 Hz, 12H$_{CH(CH3)2}$), 0.85–0.02 ppm (br m, 3H$_{BH3}$); ^{31}P{^{1}H} NMR (161 MHz, CD_2Cl_2, ppm): δ = 47.13 ppm (m); ^{13}C NMR (100 MHz, CD_2Cl_2): δ = 155.59 (d, J = 2.4 Hz, C$_{py6}$), 155.47 (d, J = 0.5 Hz, C$_{py2}$), 140.3 (s, C$_{Ar1}$), 137.08 (s, C$_{py4}$), 132.59 (s, 2C$_{Ar2,6}$), 125.44 (d, J = 2.2 Hz, C$_{py5}$), 122.90 (s, 2C$_{Ar3,5}$), 120.99 (d, J = 2.0 Hz, C$_{py3}$), 118.67 (s, C$_{Ar4}$), 46.87 (s, PyCH$_2$N), 32.98 (d, J = 25.2 Hz, PyCH$_2$P), 29.33 (d, J = 23.1 Hz, 2PC(CH$_3$)$_3$), 28.28 (d, J = 23.1 Hz, 4PC(CH$_3$)$_3$), 28.26 (s, 2ArCH(CH$_3$)$_2$), 22.59 ppm (s, 4ArCH(CH$_3$)$_2$); HRMS (FD, DCM): *m/z*: calcd for 440.3492; found: 440.3496 [M^+].

Ligand PNN^{H3}: **PNN^{H3}·BH_3** (400 mg, 0.908 mmol) was dissolved in freeze-pump-thaw degassed diethylamine (8 mL). All the volatiles were removed under vacuum after reflux for 20 h. Diethyl ether (10 mL) was added and degassed water (10 mL) was used to wash the ether solution quickly for 5 times. The ether solution was dried over sodium sulfate and the solids were filtered off. All volatiles were removed under vacuum and the ligand was obtained as a white solid (352.5 mg, 92%). ^{1}H NMR (400 MHz, CD_2Cl_2): δ = 7.55 (t, J = 7.7 Hz, 1H$_{py4}$), 7.30 (d, J = 7.8 Hz, 1H$_{py3}$), 7.11–7.09 (m, 1H$_{py5}$ +

$1H_{Ar4}$), 7.04–7.01 (m, $2H_{Ar3,5}$), 4.41 (br, $1H_{NH}$), 4.09 (s, $2H_{Py\text{-}CH2N}$), 3.43 (sept., $J=6.9$ Hz, $2H_{Ph\text{-}C(CH3)2H}$), 3.08 (d, $J=3.1$ Hz, $2H_{Py\text{-}CH2P}$), 1.23 (d, $J=7.7$ Hz, $12H_{CH(CH3)2}$), 1.17 ppm (d, $J=10.9$ Hz,$18H_{C(CH3)3}$,); $^{31}P\{^1H\}$ NMR (161 MHz, CD_2Cl_2, ppm): $\delta=35.61$ ppm; $^{13}C\{^1H\}$ NMR (100 MHz, CD_2Cl_2): $\delta=162.26$ (d, $J=14.4$ Hz, C_{Py2}), 157.72 (s, C_{Py6}), 144.39 (s, C_{Ar1}), 143.05 (s, $2C_{Ar2,6}$), 136.72 (s, C_{Py4}), 123.88 (s, C_{Ar4}), 123.81 (s, $2C_{Ar3,5}$), 122.56 (d, $J=8.5$ Hz, C_{Py3}), 118.82 (s, C_{py5}), 56.71 (Py-CH_2N), 32.13 (d, $J=23.0$ Hz, Py-CH_2P), 30.1–29.93 (s, $2PC(CH_3)_3$), 29.87 (d, $J=23.0$ Hz, $4PC(CH_3)_3$), 28.02 (s, $2ArCH(CH_3)_2$), 24.42 ppm (s, $4ArCH(CH_3)_2$); **HRMS** (FD, DCM): *m/z*: calcd for 426.3164; found: 426.3167 [M^+].

[Rh(CO)(PNN^{H3})]PF$_6$ (1): A 4 mL methanol solution of **PNN^{H3}** ligand (313.0 mg, 0.734 mmol, 2.05 equiv) was added to a 6 mL methanol solution of $[Rh(CO)_2(\mu\text{-}Cl)]_2$ (139.1 mg, 0.358 mmol, 1 equiv), followed by addition of NH_4PF_6 (466.7 mg, 2.863 mmol, 8 equiv). The solution was stirred for one hour and the concentrated to 5 mL by evacuation. The brownish-yellow precipitate was collected by filtration and washed with a small amount of cold methanol and dried in vacuo (413.8 mg, 82.3%). ^1H NMR (400 MHz, CD_2Cl_2, 225.1 K): $\delta=$ 7.96 (td, $J=9.0$, 0.9 Hz, $1H_{py4}$), 7.63 (d, $J=7.9$ Hz, $1H_{py3}$), 7.38 (d, $J=$ 7.9 Hz, $1H_{py5}$), 7.33–7.20 (br m, $3H_{aniline3,4,5}$), 6.7 (br m, $1H_{NH}$), 4.93–4.83 (br d, $J=16.6$ Hz, $1H_{Py\text{-}CHHN}$), 4.62 (dd, 17.3, 9.9 Hz, $1H_{Py\text{-}CHHN}$), 4.56–4.45 (br m, $1H_{Ph\text{-}C(CH3)2H}$), 3.78 (d, $J=9.4$ Hz, $2H_{Py\text{-}CH2P}$), 3.30–3.19 (br m, $1H_{Ph\text{-}C(CH3)2H}$), 1.59–1.23 ppm (m, $18H_{C(CH3)3}$, $12H_{CH(CH3)2}$); $^{31}P\{^1H\}$ NMR (161 MHz, CD_2Cl_2): $\delta=96.4$ ppm (d, $^1J_{Rh-P}=155.8$ Hz); $^{13}C\{^1H\}$ NMR (100 MHz, CD_2Cl_2, 225.1 K, ppm): $\delta=191.01$ (dd, $J=73.4$, 17.2 Hz, *C*O), 161.67 (t, $J=4.0$ Hz, C_{Py2}), 160.24 (s, C_{Py6}), 140.85 (s, $C_{aniline1}$), 140.54 (s, C_{Py4}), 138.12 (s, $C_{aniline2\ or\ 6}$), 127.16 (s, $2C_{aniline3,5}$), 126.29 (s, $C_{aniline6\ or\ 2}$), 123.28 (s, $C_{aniline4}$), 122.20 (d, $J=10.8$ Hz, C_{Py3}), 119.52 (s, C_{Py5}), 62.59 (s, $PyCH_2N$), 35.90 (d, $J=21.8$ Hz, $PyCH_2P$), 35.34 (dd, $J=22.9$, 2.3 Hz, $PC(CH_3)_3$), 28.98–28.22 (m, $ArCH(CH_3)_2$, $PC(CH_3)_3$), 25.22 (s, $ArCH(CH_3)_2$), 24.7822 (s, $ArCH(CH_3)_2$), 24.2522 (s, $ArCH(CH_3)_2$), 22.2522 ppm (s, $ArCH(CH_3)_2$); IR ($\tilde{\nu}_{CO}$, CD_2Cl_2) = 1996 cm^{-1}; HRMS (ESI, 243 K, DCM): *m/z*: calcd for 557.2168; found: 557.2161 [M^+]; elemental analysis calcd for (%) $C_{28}H_{43}F_6N_2OP_2Rh.2H_2O$: C 45.54, H 6.41, N 3.79; found: C 45.85, H 6.22, N 3.79.

[Rh(CO)(PNN^{H2})] (2): **Method I**: To a 1.5 mL THF solution of **1** (10.0 mg, 0.0179 mmol, 1 equiv) was added a THF solution of potassium *tert*-butoxide (1 M in THF, 0.0179 mL, 1 equiv). The solution was stirred for 5 min and the solids were filtered off. The solvent was removed under vacuum. Complex **2** was obtained as a mixture with two other species; **Method II**: To a 0.3 mL C_6D_6 suspension of **1** (5.0 mg, 0.0071 mmol, 1 equiv) was slowly added a 0.2 mL C_6D_6 solution of potassium bis(trimethylsilyl)amide (KHMDS, 1.4 mg, 0.0073 mmol, 1.02 equiv). The mixture was stirred for 5 min and the insoluble solids were filtered off and the filtrate was directly transferred to a NMR tube which was sealed afterwards. ^1H NMR (400 MHz, C_6D_6): $\delta=7.39$–7.36 (m, $1H_{aniline3,5}$), 7.28 (dd, $J=8.3$, 6.9 Hz, $1H_{aniline4}$), 6.69 (t, $J=7.7$ Hz, $1H_{py4}$), 6.44 (d, $J=7.9$ Hz, $1H_{py3}$), 6.35 (d, $J=7.7$ Hz, $1H_{py5}$), 5.29 (s, $2H_{Py\text{-}CH2N}$), 4.61 (sept, 6.8 Hz, $2H_{Ph\text{-}C(CH3)2H}$), 2.91 (d, $2H_{Py\text{-}CH2P}$), 1.71 (d, $J=6.8$ Hz, $6H_{CH(CH3)2}$), 1.50 (d, $J=$ 7.0 Hz, $6H_{CH(CH3)2}$), 1.10 ppm (d, $J=13.4$ Hz, $18H_{C(CH3)3}$); $^{31}P\{^1H\}$ NMR (161 MHz, C_6D_6, ppm): $\delta=88.1$ (d, $^1J_{Rh-P}=129.7$ Hz); HRMS (ESI, 243 K, C_6D_6): *m/z*: calcd for 557.2163; found: 557.2176 [M+H$^+$]. *Due to its inherent instability, no reliable $^{13}C\{^1H\}$ NMR data were obtained for complex **2**. Attempts to record IR spectra of complex **2** in C_6D_6 in a solution KBr cell led to detection of a CO stretch frequency of 1954 cm^{-1} in several IR measurements, thus indicating fast formation of **4** from **2** in the KBr IR cell. The observation is in agreement with the observed H_2 loss from complex **2** to form complex **4** revealed by ^1H NMR. In the KBr IR cell the transformation seems to be accelerated somehow. However, there is also a possibility that complex **2** and **4** have (nearly) identical overlapping CO stretch frequencies. The two complexes have ν_{CO} of 1954.7 (**2**) and 1953.4 cm^{-1} (**4**) according to DFT calculations at BP86/def2-TZVP level.

[Rh(CO)(PNN^{H})]PF$_6$ (3): To a 3 mL THF solution of **1** (40.0 mg, 0.0570 mmol, 1 equiv) and sodium bicarbonate ($NaHCO_3$, 23.9 mg, 0.285 mmol, 5 equiv) was added a THF solution of potassium *tert*-butoxide (*t*BuOK 1 M in THF, 0.0570 mL, 1 equiv). The solution was stirred overnight, and **3** was obtained as a mixture with **4**. The solvent was removed under vacuum. The solids were first washed with pentane (5×2 mL) and dichloromethane (2 mL) was added. The solids were filtered off. The DCM solvent was removed under vacuum. Complex **3** was obtained as a brownish-red solid (14.4 mg, 36%). Crystals suitable for X-ray diffraction were obtained by top-layering a DCM solution of **3** with diethyl ether. **^1H NMR** (400 MHz, CD_2Cl_2): $\delta=8.39$ (dd, $J=5.3$, 2.8 Hz, $1H_{PyCH=N}$), 8.21 (t, $J=$ 7.8 Hz, $1H_{Py4}$), 8.02 (d, $J=8.1$ Hz, $1H_{Py3}$), 7.97 (d, $J=7.8$ Hz, $1H_{Py5}$), 7.36 (dd, $J=8.9$, 6.4 Hz, $1H_{aniline4}$), 7.32–7.21 (m, $2H_{aniline3,5}$), 3.91 (d, $J=9.1$ Hz, $2H_{PyCH2P}$), 3.36 (sept., $J=6.7$ Hz, $2H_{CH(CH3)2}$), 1.39 (d, $J=$ 15.1 Hz, $18H_{C(CH3)3}$), 1.36 (d, $J=6.8$ Hz, $6H_{CH(CH3)2}$), 1.23 ppm (d, $J=$ 6.9 Hz, $6H_{CH(CH3)2}$); $^{31}P\{^1H\}$ NMR (161 MHz, CD_2Cl_2, ppm): $\delta=$ 96.30 ppm (d, $^1J_{Rh-P}=149.3$ Hz); $^{13}C\{^1H\}$ NMR (100 MHz, CD_2Cl): $\delta=$ 190.97 (dd, $J=73.9$, 16.6 Hz, *C*O), 168.87 (d, 2.4 Hz, $C_{PyCH=N}$), 165.29 (t, $J=4.3$ Hz, C_{Py2}), 153.75 (d, $J=2.2$ Hz, C_{Py6}), 147.01 (s, $C_{aniline1}$), 141.89 (s, C_{Py4}), 138.92 (s, $2C_{aniline2,6}$), 128.60 (s, $C_{aniline4}$), 128.06 (d, $J=$ 10.6 Hz, C_{py3}), 126.94 (s, C_{py5}), 124.32 (s, $2C_{aniline3,5}$), 37.38 (d, $J=$ 22.1 Hz, $C_{PyCH\text{-}P}$), 36.56 (dd, $J=20.6$, 1.8 Hz, $P(CH_3)_3$), 29.36 (d, $J=$ 4.5 Hz, $P(CH_3)_2$), 28.95 (s, $CH(CH_3)_2$), 24.12 (s, $CH(CH_3)_2$), 22.97 ppm (s, $CH(CH_3)_2$); IR ($\tilde{\nu}_{CO}$, CD_2Cl_2) = 2003 cm^{-1}; HRMS (ESI, 243 K, CD_2Cl_2): *m/z*: calcd for 555.2012; found 555.2035 [M^+]; elemental analysis (%) calcd for $C_{28}H_{41}F_6N_2OP_2Rh$: C 48.01, H 5.90, N 4.00; found: C 48.69, H 5.81, N 4.31.

[Rh(CO)(PNN)] (4): Complex **4** was obtained by adding THF solution of potassium *tert*-butoxide to the reaction mixture used to synthesize complex **3**, until **3** was fully converted to **4** as monitored by ^{31}P NMR. The mixture after solvent evaporation was extracted with 2 mL pentane for three times. The solvent of the combined pentane solution was removed under vacuum and a dark blue solid was obtained (29.8 mg, 94%). Dark-blue colored crystals suitable for X-ray diffraction were obtained by storing a concentrated pentane solution of **4** at −78 °C. ^1H NMR (400 MHz, C_6D_6): $\delta=$ 7.07 (m, $3H_{Ar3,4,5}$), 6.89 (dd, $J=4.6$, 2.8 Hz, $1H_{PyCH=N}$), 6.22 (d, $J=$ 9.2 Hz, $1H_{Py3}$), 6.01 (ddd, $J=8.9$, 6.4, 1.9 Hz, $1H_{Py4}$), 5.26 (d, $J=$ 6.3 Hz, $1H_{Py5}$), 3.66 (sept., $J=6.8$ Hz, $2H_{C(CH3)2H}$), 3.44 (s, $1H_{PyCH\text{-}P}$), 1.47 (d, $J=6.8$ Hz, $6H_{CH(CH3)2}$), 1.42 (d, $J=13.8$ Hz, $18H_{C(CH3)3}$), 1.07 ppm (d, $J=6.9$ Hz, $6H_{CH(CH3)2}$); $^{31}P\{^1H\}$ NMR (161 MHz, C_6D_6): $\delta=$ 89.21 ppm (d, $^1J_{Rh\text{-}P}=156.4$ Hz); $^{13}C\{^1H\}$ NMR (100 MHz, C_6D_6): $\delta=$ 195.35 (dd, $J=70.7$, 15.4, *C*O), 168.58 (d, $J=1.4$ Hz, HC=N), 167.85 (dd, $J=16.6$, 3.8 Hz, C_{py2}), 154.69 (s, C_{py6}), 148.57 (s, C_{Ar1}), 139.38 (s, $2C_{aniline2,6}$), 131.14 (s, C_{py4}), 127.10 (s, $C_{aniline4}$), 123.64 (s, $2C_{aniline3,5}$), 122.75 (d, $J=18.9$ Hz, C_{py3}), 108.99 (s, C_{py5}), 68.98 (d, $J=53.2$ Hz, Py=*C*H-P), 36.25 (dd, $J=26.2$, 1.5 Hz, $C(CH_3)_3$), 29.73 (d, $J=5.0$ Hz, $C(CH_3)_3$), 28.41 (s, $CH(CH_3)_2$), 24.21 (s, $CH(CH_3)_2$), 23.22 ppm (s, $CH(CH_3)_2$); IR ($\tilde{\nu}_{CO}$) = 1950(CD_2Cl_2), 1954 cm^{-1} (C_6D_6); HRMS (CSI, 243 K, C_6D_6): *m/z*: calcd for 555.2006; found: 555.2033 [M+H$^+$]; elemental analysis (%) calcd for $C_{28}H_{40}N_2OPRh.H_2O$: C 58.74, H 7.39, N 4.89; found: C 59.01, H 8.13, N 4.61.

[Rh(CO)(PNN′] (5): CD_2Cl_2 (0.5 mL) was added to a vial containing complex **4** (5.0 mg, 9.0 μmol, 1 equiv) and *o*-toluenesulfonamide (1.5 mg, 9.0 μmol, 1 equiv), and the solution was stirred for 5 min. The solution was used directly for spectroscopic measurements. Yellow crystals suitable for X-ray diffraction were obtained by storing a CD_2Cl_2/diethyl ether solution of **5** at −20 °C. ^1H NMR

(400 MHz, CD_2Cl_2): $\delta = 8.16$ (dd, $J = 7.8$, 1.6 Hz, $1H_{Ts6}$), 7.40 (td, $J = 7.8$ 1.0 Hz, $1H_{Py4}$), 7.28 (d, $J = 7.4$ 1.5 Hz, $1H_{Py3}$), 7.23 (td, $J = 7.8$, 1.6 Hz, $1H_{Ts4}$), 7.16 (t, $J = 7.5$ Hz, $1H_{Ts5}$), 7.10 (d, $J = 7.4$ Hz, $1H_{Ts3}$), 7.01–6.95 (m, $3H_{aniline3,4,5}$), 6.29 (d, $J = 7.7$ Hz, $1H_{Py5}$), 5.83 (dd, $J =$ 10.5, 3.1 Hz, $1H_{PyCHN}$), 3.75 (d, $J = 10.4$ Hz, $1H_{NH}$), 3.55 (d, $J = 8.9$ Hz, $2H_{PyCH2P}$), 3.03 (sept. $J = 7.0$ Hz, $2H_{CH(CH3)2}$), 2.66 (s, $3H_{Ts-CH3}$), 1.40 (d, $J = 14.3$ Hz, $9H_{P(CH3)2}$), 1.34 (d, $J = 14.2$ Hz, $9H_{P(CH3)2}$), 1.13 (d, $J =$ 6.8 Hz, $9H_{CH(CH3)2}$), 0.87 ppm (d, $J = 6.7$ Hz, $9H_{CH(CH3)2}$).); $^{31}P\{^1H\}$ NMR (161 MHz, CD_2Cl_2): $\delta = 94.24$ ppm (d, $^1J_{Rh\text{-}P} = 149.3$ Hz); $^{13}C\{^1H\}$ NMR (100 MHz, CD_2Cl_2): $\delta = 193.63$ (dd, $J = 73.6$, 17.8 Hz, *C*O), 165.08 (s, C_{Py6}), 161.91 (dd, $J = 5.8$, 3.3 Hz,, C_{Py2}), 143.85 (s, $C_{quant\text{-}Ar}$), 143.11 (s, $C_{quant\text{-}Ar}$), 138.57 (s, $C_{quant\text{-}Ar}$), 137.94 (s, C_{Py4}), 136.65 (s, $C_{quant\text{-}Ar}$), 131.63 (s, C_{Ts3}), 130.29 (s, C_{Ts4}), 128.81 (s, C_{Ts6}), 125.11 (s, C_{Ts5}), 124.24 (s, $C_{aniline4}$), 123.36 (s, $C_{aniline3,5}$), 121.05 (d, $J = 10.7$ Hz, C_{Py5}), 118.69 (s, C_{Py3}), 82.72 (s, Py*C*HN), 36.01 (dd, $J = 20.2$, 4.5 Hz, PyCH_2P), 35.21 (dd, $J = 22.0$, 1.7 Hz, P*C*$(CH_3)_3$), 28.74 (dd, $J = 10.3$, 4.8 Hz, PC$(CH_3)_3$), 27.51 (s, Ar*C*H$(CH_3)_2$), 24.19 (s, ArCH$(CH_3)_2$), 23.35 (brs, ArCH$(CH_3)_2$), 21.44 ppm (s, CH_3 $_{Ts\text{-}Me}$); IR ($\tilde{\nu}_{CO}$, CD_2Cl_2) = 1983 cm^{-1}; HRMS (ESI, negative ion mode, 243 K, CD_2Cl_2): *m/z*: calcd for 724.2209; found: 724.2250 [$M-H^+$]; HRMS (ESI, positive ion mode, 243 K, CD_2Cl_2): *m/z*: calcd for 555.2006; found: 555.2033 [$M+H^+$].

[Rh(CO)(OH PNN^{H1})] (8): A wet THF solution of complex **5** (6.5 mg, 0.0179 mmol, 1 equiv) in an NMR tube was left standing for two weeks, whereafter a light yellow precipitate had formed. The solution was decanted and the yellow solid was washed four times with small amounts of THF and then dried under vacuum. ^1H NMR (400 MHz, CD_2Cl_2): $\delta = 8.21$ (dd, $J = 7.9$, 1.3 Hz, $1H_{Ts6}$), 7.76 (t, $J =$ 7.8 Hz, $1H_{Py4}$), 7.40 (d, $J = 7.8$ Hz, $1H_{Py3}$), 7.34–7.31 (m, $1H_{Py5} + 1H_{Ts4}$), 7.25–7.18 (m, $1H_{Ts5} + 1H_{Ts3}$), 6.12 (m, $1H_{PyCHN}$), 4.29 (d, $J = 2.5$ Hz, $1H_{OH}$), 3.56 (dd, $J = 9.2$, 5.2 Hz, $2H_{PyCH2P}$), 3.03 (sept. $J = 7.0$ Hz, $2H_{CH(CH3)2}$), 2.87 (s, $3H_{Ts-CH3}$), 1.36 (d, $J = 14.3$ Hz, $9H_{P(CH3)2}$), 1.36 ppm (d, $J = 14.2$ Hz, $9H_{P(CH3)2}$); $^{31}P\{^1H\}$ NMR (161 MHz, CD_2Cl_2): $\delta = 94.36$ (d, $^1J_{Rh\text{-}P} = 151.1$ Hz); $^{13}C\{^1H\}$ NMR (100 MHz, CD_2Cl_2): $\delta = 193.69$ (d, $J = 73.7$, 18.5 Hz, *C*O), 166.30 (d, $J = 1.0$ Hz, C_{Py6}), 161.25 (dd, $J = 5.9$, 3.0 Hz, C_{Py2}), 142.36 (s, C_{Ar1}), 139.54 (s, C_{Py4}), 137.69 (s, C_{Ar2}), 132.48(s, C_{Ar5}), 131.00 (s, C_{Ar4}), 128.97 (s, C_{Ar6}), 125.45 (s, C_{Ar3}), 121.92 (d, $J =$ 10.4 Hz, C_{Py3}), 121.64(s, C_{Py5}), 90.15 (s, Py*C*H(OH)NTs), 36.56 (d, $J =$ 20.0 Hz, PyCH_2P), 36.03 (td, $J = 18.9$, 1.7 Hz, P*C*$(CH_3)_3$), 29.25 (d, $J =$ 4.8 Hz, 2PC$(CH_3)_3$), 21.97 (s, $C_{Ts\text{-}CH3}$); IR ($\tilde{\nu}_{CO}$, CD_2Cl_2 + (trace) [D_4]MeOH) = 1984 cm^{-1}; HRMS (ESI, negative ion mode, 243 K, CD_2Cl_2 + (trace) [D_4]MeOH): *m/z*: calcd for 565.0803; found: 565.0811 [$M-H^+$]; HRMS (ESI, positive ion mode, 243 K, CD_2Cl_2): *m/z*: calcd for 549.0848; found: 549.0909 [M^+] (complex **7**).

[Rh(CO)(*o*Ts *o*Ts PNN^{H1})] (9): 0.5 mL CD_2Cl_2 was added to a vial containing complex **4** (5.0 mg, 9.0 μmol, 1 equiv) and *o*-toluenesulfonamide (3.9 mg, 22.5 μmol, 2.5 equiv), and the solution was transferred to a sealed NMR tube. The solution was heated at 50 °C for six hours. ^1H NMR (400 MHz, CD_2Cl_2, ppm): $\delta = 8.04$ (dd, $J = 8.2$, 1.4 Hz, $1H_{Ts(1)6}$), 7.85 (d, $J = 7.9$ Hz, $1H_{Ts(2)6}$), 7.68 (t, $J = 7.8$ Hz, $1H_{Py4}$), 7.51–7.47 ($1H_{Ts(1)4}$), 7.49–7.45 ($1H_{Py3}$), 7.36–7.34 ($1H_{Py5}$), 7.32–7.28 (m, $2H_{Ts(1)3,5}$), 7.24 (td, $J = 7.3$, 1.5 Hz, $1H_{Ts(2)4}$), 7.11–7.06 (m, $2H_{Ts(2)3,5}$), 6.03 (brs, $1H_{PyCHN}$), 5.77 (brs, $1H_{NH}$), 3.52 (d, $J = 9.1$ Hz, $2H_{PyCH2P}$), 2.66 (s, $3H_{Ts(1)\text{-}CH3}$), 2.56 (s, $3H_{Ts(2)\text{-}CH3}$), 1.37 (d, $J = 14.3$ Hz, $9H_{P(CH3)3}$), 1.26 (d, $J = 14.4$ Hz, $9H_{P(CH3)3}$); $^{31}P\{^1H\}$ NMR (161 MHz, CD_2Cl_2): $\delta = 94.11$ ppm (d, $^1J_{Rh\text{-}P} = 151.3$ Hz); $^{13}C\{^1H\}$ NMR (100 MHz, CD_2Cl_2): $\delta = 193.31$ (dd, $J = 73.9$, 18.1 Hz, *C*O), 165.26 (s, C_{Py6}), 161.52 (dd, $J = 73.9$, 18.1 Hz, C_{Py2}), 143.06 (s, C_{Ar}), 140.11 (s, C_{Ar}), 139.23 (s, C_{Ar}), 137.84, (s, C_{Ar}), 132.80 (s, C_{Ar}), 132.56 (s, C_{Ar}), 132.21 (s, C_{Ar}), 130.84 (s, C_{Ar}), 129.99 (s, $C_{Ts(1)6}$), 128.91 (s, $C_{Ts(2)6}$), 126.03 (s, C_{Ar}), 125.44 (s, C_{Ar}), 121.70 (d, $J = 10.8$ Hz, C_{Py3}), 121.53 (s, C_{Py5}), 78.83 (s, Py*C*HN), 36.56 (d, $J =$ 20.1 Hz, PyCH_2P), 36.09 (d, $J = 19.7$ Hz, P*C*$(CH_3)_3$), 35.76 (dd, $J = 21.9$, 1.8 Hz, P*C*$(CH_3)_3$), 29.21–19.14 (m, 2PC$(CH_3)_3$), 21.40 (s, $C_{Ts2\text{-}CH3}$), 20.78 ppm (s, $C_{Ts1\text{-}CH3}$); IR ($\tilde{\nu}_{CO}$, CD_2Cl_2) = 1985 cm^{-1}; HRMS (ESI, negative, 243 K, CD_2Cl_2): *m/z*: calcd for 718.1051; found: 718.1452 [$M-H^+$]; HRMS (ESI, positive ion mode, 243 K, CD_2Cl_2): *m/z*: calcd for 549.0848; found: 549.0747 [M^+] (complex **7**).

[Rh(CO)(PNN^H)]I (3′): 55% Hydriodic acid (HI, 2.0 μL, 0.0146 mmol, 2 equiv) was added to a CD_2Cl_2 solution (0.5 mL) of complex **4** (4.0 mg, 0.0072 mmol, 1 equiv) in a NMR tube. ^1H NMR (400 MHz, CD_2Cl_2): $\delta = 8.60$ (dd, $J = 5.4$, 2.7 Hz, $1H_{PyCH=N}$), 8.32–8.30 (m, $1H_{Py4} + 1H_{Py3}$), 8.20–8.19 (m, $1H_{Py5}$), 7.37–7.28 (m, $3H_{Ar3,4,5}$), 4.13 (dd, $J = 8.9$, 2.1 Hz, $2H_{PyCH2P}$), 3.37 (sept., $J = 6.8$ Hz, $2H_{CH(CH3)2}$), 1.41 (d, $J =$ 15.0 Hz, $18H_{C(CH3)3}$), 1.36 (d, $J = 6.8$ Hz, $6H_{CH(CH3)2}$), 1.23 ppm (d, $J =$ 6.9 Hz, $6H_{CH(CH3)2}$); $^{31}P\{^1H\}$ NMR (161 MHz, CD_2Cl_2, ppm): $\delta = 96.72$ (d, $^1J_{Rh\text{-}P} = 149.2$ Hz); $^{13}C\{^1H\}$ NMR (100 MHz, CD_2Cl_2): $\delta = 168.87$ (d, 2.4 Hz, $C_{PyCH=N}$), 165.29 (t, $J = 4.3$ Hz, C_{Py2}), 153.75 (d, $J = 2.2$ Hz, C_{Py6}), 147.01 (s, $C_{aniline1}$), 141.89 (s, C_{Py4}), 138.92 (s, $2C_{aniline2,6}$), 128.60 (s, $C_{aniline4}$), 128.06 (d, $J = 10.6$ Hz, C_{py3}), 126.94 (s, C_{py5}), 124.32 (s, $2C_{aniline3,5}$), 37.38 (d, $J = 22.1$ Hz, C_{PyCH-P}), 36.56 (dd, $J = 20.6$, 1.8 Hz, $P(CH_3)_3$), 29.36 (d, $J = 4.5$ Hz, $P(CH_3)_2$), 28.95 (s, *C*H$(CH_3)_2$), 24.12 (s, CH$(CH_3)_2$), 22.97 ppm (s, CH$(CH_3)_2$); IR($\tilde{\nu}_{CO}$, CD_2Cl_2) = 2003 cm^{-1}; HRMS (ESI, 243 K, DCM): *m/z*: calcd for 555.2012; found: 555.2094. *The CO carbon resonance signal was not observable in ^{13}C NMR spectra, but this complex is only used to confirm the expected product formation in the coupling reaction (Scheme S1). The other peaks in ^{13}C NMR are identical to those of complex **3**, which are compared and mentioned in Figure S62.

***N*,2-Dimethylbenzene sulfonamide (*o*TsNHMe)**: To a MeOH solution (4 mL) of sodium (*o*-tolylsulfonyl)amide (53.3 mg, 0.276 mmol, 1 equiv) was added iodomethane (MeI, 20.6 μL, 0.331 mmol, 1.2 equiv), the solution was stirred for 16 h. The volatiles were removed by rota-evaporation. CD_2Cl_2 was directly added to dissolve out the product. After filtration, the filtrate was taken for NMR and HRMS measurements. ***o*TsNH$_2$** and ***o*TsNMe$_2$** were found as impurities in 15% and 27%. ^1H NMR (400 MHz, CD_2Cl_2): $\delta = 7.92$ (dd, $J =$ 8.3, 1.5 Hz, $1H_{Ar6}$), 7.49 (td, $J = 7.5$, 1.5 Hz, $1H_{Ar4}$), 7.36–7.32 (m, $2H_{Ar3,5}$), 2.62 (s, $3H_{ArCH3}$), 2.59 ppm (s, $3H_{NCH3}$); $^{13}C\{^1H\}$ NMR (100 MHz, CD_2Cl_2, ppm): $\delta = 137.44$ (s, C_{Ar1}), 137.19 (s, C_{Ar2}), 133.14 (s, C_{Ar4}), 132.96 (s, C_{Ar3}), 130.04 (s, C_{Ar6}), 126.51 (s, C_{Ar5}), 29.31 (s, C_{NCH3}), 20.42 ppm (s, C_{ArCH3}); HRMS (FD, DCM): *m/z*: calcd for 184.0510; found: 185.0522 [M^+].

X-ray crystallography: X-ray intensities were measured on either a Bruker Venture D8 (complex **4**) or on a Bruker D8 Quest Eco diffractometer equipped with a Triumph monochromator ($\lambda =$ 0.71073 Å). Diffraction data were collected at 150(2) K using a CMOS Photon 50 detector (complexes **1**, **3** and **5**) or at 100(2) K using a CMOS Photon 100 detector (complex **4**). Intensity data were integrated with Bruker APEX2 (complex **4**) or the Bruker APEX software (complexes **1**, **3** and **5**).[26] Absorption correction and scaling was performed with SADABS.[27] The structures were solved using direct methods with SHELXS-97 (complex **4**) or SHELXL-13[28] (complexes **1**, **3** and **5**). Least-squares refinement was performed with SHELXL-2014 (complex **4**) or SHELXL-2013[28] (complexes **1**, **3** and **5**) against F^2 of all reflections. Non-hydrogen atoms were refined with anisotropic displacement parameters. Heteroatom bound hydrogen atoms were refined freely with an isotropic displacement parameter, all other hydrogen atoms were included at calculated positions using a riding model. Geometry calculations and checking for higher symmetry was performed with the PLATON program.[29]

Crystallographic details for 1: $C_{28}H_{43}N_2OP_2Rh$, $F_w = 702.49$, yellow-golden rectangles, $0.574 \times 0.118 \times 0.113$ mm^3, monoclinic, $P2_1/n$, $a =$ 11.6022(4), $b = 13.8309(5)$, $c = 21.1322(9)$ Å, $\beta = 94.828(2)°$, $V =$ 3379.0(2) $Å^3$, $Z = 4$, $\rho_x = 1.381$ g cm^{-3}, $\mu = 0.656$ mm^{-1}. 28807 reflections were measured up to a resolution of $2(\sin\theta/\lambda)_{max} = 1.26$ $Å^{-1}$. 5947 Reflections were unique ($R_{int} = 0.0600$), of which 4606 were

observed [$I>2\sigma(I)$]. 459 Parameters were refined with 307 restraints. $R1/wR2$ [$I>2\sigma(I)$]: 0.0340/0.0708. $R1/wR2$ [all refl.]: 0.0553/0.0782. $S=1.030$. CCDC 1048612 contains the supplementary crystallographic data for this paper. These data can be obtained free of charge from The Cambridge Crystallographic Data Centre.

Crystallographic details for 3: $C_{28}H_{41}N_2OP_2Rh\ PF_6$, $F_w=700.48$, red-brown block, $0.3\times0.2\times0.1\ mm^3$, triclinic, $P\bar{1}$, $a=8.6285(4)$, $b=12.1541(5)$, $c=16.6555(7)$ Å, $\alpha=69.373(2)$, $\beta=76.414(2)$, $\gamma=78.091(2)^\circ$, $V=1574.24(12)$ Å^3, $Z=2$, $\rho_x=1.407\ g\,cm^{-3}$, $\mu=0.704\ mm^{-1}$. 45078 Reflections were measured up to a resolution of $2(\sin\theta/\lambda)_{max}=1.37$ Å^{-1}. 5696 Reflections were unique ($R_{int}=0.0541$), of which 4971 were observed [$I>2\sigma(I)$]. 444 Parameters were refined with no restraints. $R1/wR2$ [$I>2\sigma(I)$]: 0.0267/0.0579. $R1/wR2$ [all refl.]: 0.0357/0.0615. $S=1.109$. CCDC 1048613 contains the supplementary crystallographic data for this paper. These data can be obtained free of charge from The Cambridge Crystallographic Data Centre.

Crystallographic details for 4: $C_{28}H_{40}N_2OPRh$, $F_w=554.50$, dark green block, $0.38\times0.38\times0.12$ mm, monoclinic, $P2_1/c$, $a=15.1902(6)$, $b=10.4618(4)$, $c=17.4934(6)$ Å, $\beta=96.1846(18)^\circ$, $V=2763.82(18)$ Å^3, $Z=4$, $\rho_x=1.333\ g\,cm^{-3}$, $\mu=0.697\ mm^{-1}$. 32777 Reflections were measured up to a resolution of $2(\sin\theta/\lambda)_{max}=1.31$ Å^{-1}. 6546 Reflections were unique ($R_{int}=0.0269$), of which 5768 were observed [$I>2\sigma(I)$]. 308 Parameters were refined with no restraints. $R1/wR2$ [$I>2\sigma(I)$]: 0.0256/0.0598. $R1/wR2$ [all refl.]: 0.0324/0.0598. S = 1.061. CCDC 1049097 contains the supplementary crystallographic data for this paper. These data can be obtained free of charge from The Cambridge Crystallographic Data Centre.

Crystallographic details for 5: $C_{35}H_{49}N_3O_3PRhS\ CH_2Cl_2$, Fw = 810.63, yellow block, $0.4\times0.2\times0.1\ mm^3$, monoclinic, $P2_1/n$, $a=11.2583(4)$, $b=13.6561(5)$, $c=25.5029(10)$ Å, $\beta=102.5430(18)^\circ$, $V=3827.4(2)$ Å^3, $Z=4$, $\rho_x=1.407\ g\,cm^{-3}$, $\mu=0.720\ mm^{-1}$. 26791 Reflections were measured up to a resolution of $2(\sin\theta/\lambda)_{max}=1.67$ Å^{-1}. 6749 Reflections were unique ($R_{int}=0.0398$), of which 5946 were observed [$I>2\sigma(I)$]. 438 Parameters were refined with no restraints. $R1/wR2$ [$I>2\sigma(I)$]: 0.0295/0.0767. $R1/wR2$ [all refl.]: 0.0359/0.0875. $S=1.108$. CCDC 1048614 contains the supplementary crystallographic data for this paper. These data can be obtained free of charge from The Cambridge Crystallographic Data Centre.

DFT calculations: The gas phase geometries of the complexes **3** and **4** were optimized with the Turbomole program package[30] coupled to the PQS Baker optimizer[31] via the BOpt package[32] at the ri-DFT[33]/BP86[34] level. We used the def2-TZVP basis set[35] for all atoms and a small grid (m4). The minima (no imaginary frequencies) were characterized by calculating the Hessian matrix. The Cartesian coordinates of the optimized geometries are supplied as a separated zip file (.pdb and.xyz format). Orbital plots were generated using the program VMD 1.9.1.[36]

Acknowledgements

This research was funded by the Netherlands Organization for Scientific Research, sections Chemical Sciences (NWO-CW; ECHO & VICI grant to B.B.). J.I.V. thanks the ERC for a Starting Grant (279097, EuReCat) and Dr. M. A. Siegler (John Hopkins University) for tips and tricks regarding X-ray structure refinement.

Keywords: amine activation · cooperative reactivity · pincer · reactive ligand · rhodium · sulfonamide

[1] a) D. Morales-Morales, C. M. Jensen, *The Chemistry of Pincer Compounds*, Elsevier, Amsterdam, **2007**; b) G. van Koten, D. Milstein, *Top. Organomet. Chem. Vol. 40* Springer, Heidelberg, **2013**.

[2] a) H. Grützmacher, *Angew. Chem. Int. Ed.* **2008**, *47*, 1814 – 1818; *Angew. Chem.* **2008**, *120*, 1838 – 1842; b) J. I. van der Vlugt, J. N. H. Reek, *Angew. Chem. Int. Ed.* **2009**, *48*, 8832 – 8848; *Angew. Chem.* **2009**, *121*, 8990 – 9004; c) R. H. Crabtree, *New J. Chem.* **2011**, *35*, 18 – 23; d) C. Gunanathan, D. Milstein, *Acc. Chem. Res.* **2011**, *44*, 588 – 602; e) T. Ikariya, K. Murata, R. Noyori, *Org. Biomol. Chem.* **2006**, *4*, 393 – 406.

[3] a) G. E. Dobereiner, R. H. Crabtree, *Chem. Rev.* **2010**, *110*, 681 – 703; b) G. Guillena, D. J. Ramon, M. Yus, *Chem. Rev.* **2010**, *110*, 1611 – 1641; c) C. Gunanathan, D. Milstein, *Science* **2013**, *341*, 249 – 260.

[4] a) J. I. van der Vlugt, *Eur. J. Inorg. Chem.* **2012**, 363 – 375; b) R. H. Morris, *Chem. Soc. Rev.* **2009**, *38*, 2282 – 2291; c) K. Junge, K. Schröder, M. Beller, *Chem. Commun.* **2011**, *47*, 4849 – 4859.

[5] For other cooperative ligand types, see: a) R. Noyori, S. Hashiguchi, *Acc. Chem. Res.* **1997**, *30*, 97 – 102; b) Y. Blum, Y. Shvo, *J. Organomet. Chem.* **1985**, *282*, C7 – 10; c) T. Zweifel, J.-V. Naubron, H. Grützmacher, *Angew. Chem. Int. Ed.* **2009**, *48*, 559 – 563; *Angew. Chem.* **2009**, *121*, 567 – 571; d) M. Königsmann, N. Donati, D. Stein, H. Schönberg, J. Harmer, A. Sreekanth, H. Grützmacher, *Nat. Chem.* **2013**, *5*, 342 – 347; e) W. Zuo, A. J. Lough, Y. F. Li, R. H. Morris, *Science* **2013**, *342*, 1080 – 1083; f) S. Kuwata, T. Ikariya, *Chem. Eur. J.* **2011**, *17*, 3542 – 3556; g) D. Spasyuk, S. Smith, D. G. Gusev, *Angew. Chem. Int. Ed.* **2012**, *51*, 2772 – 2775; *Angew. Chem.* **2012**, *124*, 2826 – 2829; h) E. Putignano, G. Bossi, P. Rigo, W. Baratta, *Organometallics* **2012**, *31*, 1133 – 1142; i) D. V. Gutsulyak, W. E. Piers, J. Borau-Garcia, M. Parvez, *J. Am. Chem. Soc.* **2013**, *135*, 11776 – 11779; j) C. M. Moore, N. K. Szymczak, *Chem. Commun.* **2013**, *49*, 400 – 402; k) R. Kawahara, K.-i. Fujita, R. Yamaguchi, *Angew. Chem. Int. Ed.* **2012**, *51*, 12790 – 12794; *Angew. Chem.* **2012**, *124*, 12962 – 12966; m) F. W. Patureau, M. Kuil, A. J. Sandee, J. N. H. Reek, *Angew. Chem. Int. Ed.* **2008**, *47*, 3180 – 3183; *Angew. Chem.* **2008**, *120*, 3224 – 3227; n) S. Oldenhof, B. de Bruin, M. Lutz, F. W. Patureau, J. I. van der Vlugt, J. N. H. Reek, *Chem. Eur. J.* **2013**, *19*, 11507 – 11511; o) Y. Gloaguen, W. Jacobs, J. N. H. Reek, M. Lutz, B. de Bruin, J. I. van der Vlugt, *Inorg. Chem.* **2013**, *52*, 1682 – 1684.

[6] a) E. Ben Ari, G. Leitus, L. J. W. Shimon, D. Milstein, *J. Am. Chem. Soc.* **2005**, *127*, 10840 – 10841; b) C. Gunanathan, Y. Ben-David, D. Milstein, *Science* **2007**, *317*, 790 – 792; c) S. W. Kohl, L. Weiner, L. Schwartsburd, L. Konstantinovski, L. J. W. Shimon, Y. Ben-David, M. A. Iron, D. Milstein, *Science* **2009**, *324*, 74 – 77; d) J. I. van der Vlugt, M. Lutz, E. A. Pidko, D. Vogt, A. L. Spek, *Dalton Trans.* **2009**, 1016 – 1023; e) B. Gnanaprakasam, D. Milstein, *J. Am. Chem. Soc.* **2011**, *133*, 1682 – 1685; f) E. Balaraman, C. Gunanathan, J. Zhang, L. J. W. Shimon, D. Milstein, *Nat. Chem.* **2011**, *3*, 609 – 614; g) J. I. van der Vlugt, E. A. Pidko, R. C. Bauer, Y. Gloaguen, M. K. Rong, M. Lutz, *Chem. Eur. J.* **2011**, *17*, 3850 – 3854; h) E. Balaraman, E. Khaskin, G. Leitus, D. Milstein, *Nat. Chem.* **2013**, *5*, 122 – 125; i) Y. Gloaguen, C. Rebreyend, M. Lutz, P. Kumar, M. Huber, J. I. van der Vlugt, S. Schneider, B. de Bruin, *Angew. Chem. Int. Ed.* **2014**, *53*, 6814 – 6814; *Angew. Chem.* **2014**, *126*, 6932 – 6936.

[7] a) S. Y. de Boer, Y. Gloaguen, J. N. H. Reek, M. Lutz, J. I. van der Vlugt, *Dalton Trans.* **2012**, *41*, 11276 – 11283; b) S. Y. de Boer, Y. Gloaguen, M. Lutz, J. I. van der Vlugt, *Inorg. Chim. Acta* **2012**, *380*, 336 – 342.

[8] For similar systems but with -NH spacers, see: a) D. Benito-Garagorri, K. Kirchner, *Acc. Chem. Res.* **2008**, *41*, 201 – 213; b) D. Benito-Garagorri, M. Puchberger, K. Mereiter, K. Kirchner, *Angew. Chem. Int. Ed.* **2008**, *47*, 9142 – 9145; *Angew. Chem.* **2008**, *120*, 9282 – 9285; c) N. Gorgas, B. Stöger, L. F. Veiros, E. Pittenauer, G. Allmaier, K. Kirchner, *Organometallics* **2014**, *33*, 6905 – 6914; d) M. Glatz, B. Bichler, M. Mastalir, B. Stöger, M. Weil, K. Mereiter, E. Pittenauer, G. Allmaier, L. F. Veiros, K. Kirchner, *Dalton Trans.* **2015**, *44*, 281 – 294; e) H. Li, B. Zheng, K.-W. Huang, *Coord. Chem. Rev.* **2015**, *293 – 294*, 116 – 138; f) L.-P. He, T. Chen, D. Gong, Z. Lai, K.-W. Huang, *Organometallics* **2012**, *31*, 5208 – 5211.

[9] a) Y. Gumrukcu, B. de Bruin, J. N. H. Reek, *ChemSusChem* **2014**, *7*, 890 – 896; b) W. I. Dzik, X. Xu, X. P. Zhang, J. N. H. Reek, B. de Bruin, *J. Am. Chem. Soc.* **2010**, *132*, 10891 – 10902; c) K. Gruet, E. Clot, O. Eisenstein, D. H. Lee, B. Patel, A. Macchioni, R. H. Crabtree, *New J. Chem.* **2003**, *27*, 80 – 87.

[10] a) W. H. Harman, J. C. Peters, *J. Am. Chem. Soc.* **2012**, *134*, 5080 – 5082; b) H. Fong, M.-E. Moret, Y. Lee, J. C. Peters, *Organometallics* **2013**, *32*, 3053 – 3062; c) G. Zeng, S. Sakaki, *Inorg. Chem.* **2013**, *52*, 2844 – 2853; d) S. N. MacMillan, W. H. Harman, J. C. Peters, *Chem. Sci.* **2014**, *5*, 590 –

597; e) N. Curado, C. Maya, J. López-Serrano, A. Rodríguez, *Chem. Commun.* **2014**, *50*, 15718 – 15721; f) W. H. Harman, T.-P. Lin, J. C. Peters, *Angew. Chem. Int. Ed.* **2014**, *53*, 1081 – 1086; *Angew. Chem.* **2014**, *126*, 1099 – 1104. One report involving direct substrate-to-(imine)ligand hydride transfer, but only as a catalyst-activating step: g) A. Mikhailine, M. I. Maishan, A. J. Lough, R. H. Morris, *J. Am. Chem. Soc.* **2012**, *134*, 12266 – 12280. Alternatively, as a catalyst-deactivation initiating step: h) D. E. Prokopchuk, J. F. Sonnenberg, N. Meyer, M. Z.-D. Iuliis, A. J. Lough, R. H. Morris, *Organometallics* **2012**, *31*, 3056 – 3064.

[11] For reviews, see: a) V. Lyaskovskyy, B. de Bruin, *ACS Catal.* **2012**, *2*, 270 – 279; b) O. R. Luca, R. H. Crabtree, *Chem. Soc. Rev.* **2013**, *42*, 1440 – 1459; For selected examples, see: c) P. Chaudhuri, M. Hess, U. Flörke, K. Wieghardt, *Angew. Chem. Int. Ed.* **1998**, *37*, 2217 – 2220; *Angew. Chem.* **1998**, *110*, 2340 – 2343; d) P. Chaudhuri, M. Hess, J. Müller, K. Hildenbrand, E. Bill, T. Weyhermüller, K. Wieghardt, *J. Am. Chem. Soc.* **1999**, *121*, 9599 – 9610; e) K. Tsuge, M. Kurihara, K. Tanaka, *Bull. Chem. Soc. Jpn.* **2000**, *73*, 607 – 614; f) M. Königsmann, N. Donati, D. Stein, H. Schönberg, J. Harmer, A. Sreekanth, H. Grützmacher, *Angew. Chem. Int. Ed.* **2007**, *46*, 3567 – 3570; *Angew. Chem.* **2007**, *119*, 3637 – 3640; g) D. L. J. Broere, B. de Bruin, J. N. H. Reek, M. Lutz, J. I. van der Vlugt, *J. Am. Chem. Soc.* **2014**, *136*, 11574 – 11577; h) D. L. J. Broere, L. L. Metz, B. de Bruin, J. N. H. Reek, M. A. Siegler, J. I. van der Vlugt, *Angew. Chem. Int. Ed.* **2015**, *54*, 1516 – 1520; *Angew. Chem.* **2015**, *127*, 1536 – 1540.

[12] For a conceptually different ligand system cooperating in *either* aniline splitting and (permanent)storage *or* thiol splitting in typical (Lewis) acid metal-basic ligand manner for further coupling: a) A. Scharf, I. Goldberg, A. Vigalok, *Inorg. Chem.* **2014**, *53*, 12 – 14. For another ligand system involving electronic-activation and temporary storage of substrates as electrophiles for further outer-sphere coupling, see: b) M. Vogt, A. Nerush, M. A. Iron, G. Leitus, Y. Diskin-Posner, L. J. W. Shimon, Y. Ben-David, D. Milstein, *J. Am. Chem. Soc.* **2013**, *135*, 17004 – 17018; c) S. Perdriau, D. S. Zijlstra, H. J. Heeres, J. G. de Vries, E. Otten, *Angew. Chem. Int. Ed.* **2015**, *54*, 4236 – 4240; *Angew. Chem.* **2015**, *127*, 4310 – 4314.

[13] a) C. Tejel, M. A. Ciriano, M. P. del Río, F. J. van den Bruele, D. G. H. Hetterscheid, N. Tsichlis i Spithas, B. de Bruin, *J. Am. Chem. Soc.* **2008**, *130*, 5844 – 5845; b) C. Tejel, M. P. del Río, L. Asensio, F. J. van den Bruele, M. A. Ciriano, N. Tsichlis i Spithas D. G. H. Hetterscheid, B. de Bruin, *Inorg. Chem.* **2011**, *50*, 7524 – 7534; c) C. Tejel, L. Asensio, M. A. Ciriano, J. A. López, B. de Bruin, M. P. del Río, *Angew. Chem. Int. Ed.* **2011**, *50*, 8839 – 8843; *Angew. Chem.* **2011**, *123*, 9001 – 9005.

[14] J. Gómez, G. García-Herbosa, J. V. Cuevas, A. Arnáiz, A. Carbayo, A. Muñoz, L. Falvello, P. E. Fanwick, *Inorg. Chem.* **2006**, *45*, 2483 – 2493.

[15] a) M. Gargir, Y. Ben-David, G. Leitus, Y. Diskin-Posner, L. J. W. Shimon, D. Milstein, *Organometallics* **2012**, *31*, 6207 – 6214; While this manuscript was in preparation, Milstein reported a similar but not identical synthetic procedure for $\mathbf{L}^{\mathbf{H2}}$: b) E. Fogler, J A. Garg, P. Hu, G. Leitus, L. J. W. Shimon, D. Milstein, *Chem. Eur. J.* **2014**, *20*, 15727 – 15731.

[16] For related trans-effects on the Rh-P coupling constant, see: L. S. Jongbloed, B. de Bruin, J. N. H. Reek, M. Lutz, J. I. van der Vlugt, *Chem. Eur. J.* **2015**, *21*, 7297 – 7305. Two other minor species were also observed, one was later determined to be complex **4** and the other was presumably a monoanionic Rh^{I} complex with a dearomatized amido $\mathbf{PNN}^{\mathbf{H}}$ ligand, see ref. [13b], as indicated by ^{1}H and ^{31}P NMR spectra.

[17] Q. Liu, L. Wu, S. Gülak, N. Rockstroh, R. Jackstell, M. Beller, *Angew. Chem. Int. Ed.* **2014**, *53*, 7085 – 7088; *Angew. Chem.* **2014**, *126*, 7205 – 7208.

[18] a) J. I. van der Vlugt, E. A. Pidko, M. Lutz, D. Vogt, A. L. Spek, *Inorg. Chem.* **2008**, *47*, 4442 – 4444; b) J. I. van der Vlugt, E. A. Pidko, M. Lutz, D. Vogt, A. L. Spek, A. Meetsma, *Inorg. Chem.* **2009**, *48*, 7513 – 7515.

[19] a) G. A. Filonenko, M. P. Conley, C. Copéret, M. Lutz, E. J. Hensen, E. A. Pidko, *ACS Catal.* **2013**, *3*, 2522 – 2526; b) G. A. Filonenko, E. Cosimi, L. Lefort, M. P. Conley, C. Copéret, E. J. M. Hensen, E. A. Pidko, *ACS Catal.* **2014**, *4*, 2667 – 2671.

[20] Similar ligand systems but with only the metal acting as the Lewis acid, see: a) T. W. Myers, L. A. Berben, *J. Am. Chem. Soc.* **2013**, *135*, 9988 – 9990; b) T. W. Myers, L. A. Berben, *Chem. Sci.* **2014**, *5*, 2771 – 2777; c) Y.-H. Chang, Y. Nakajima, H. Tanaka, K. Yoshizawa, F. Ozawa, *J. Am. Chem. Soc.* **2013**, *135*, 11791 – 11794; d) Y.-H. Chang, Y. Nakajima, H. Tanaka, K. Yoshizawa, F. Ozawa, *Organometallics* **2014**, *33*, 715 – 721.

[21] A. Martínez-Asencio, D. J. Ramón, M. Yus, *Tetrahedron Lett.* **2010**, *51*, 325 – 328.

[22] a) J. N. H. Reek, S. Otto, *Dynamic Combinatorial Chemistry*, Wiley-VCH, Weinheim, **2010**; b) J.-M. Lehn, *Chem. Eur. J.* **1999**, *5*, 2455 – 2463; c) S. J. Rowan, S. J. Cantrill, G. R. L. Cousins, J. K. M. Sanders, J. F. Stoddart, *Angew. Chem. Int. Ed.* **2002**, *41*, 898 – 952; *Angew. Chem.* **2002**, *114*, 938 – 993; d) J. R. Nitschke, *Acc. Chem. Res.* **2007**, *40*, 103 – 112; e) J. Li, P. Nowak, S. Otto, *J. Am. Chem. Soc.* **2013**, *135*, 9222 – 9239; f) J. K. M. Sanders, *Chem. Eur. J.* **1998**, *4*, 1378 – 1383; g) P. T. Corbett, J. Leclaire, L. Vial, K. R. West, J.-L. Wietor, J. K. M. Sanders, S. Otto, *Chem. Rev.* **2006**, *106*, 3652 – 3711.

[23] a) J. L. García Ruano, A. Parra, J. Alemán, F. Yuste, V. M. Mastranzo, *Chem. Commun.* **2009**, 404 – 406; b) C. W. Cheung, D. S. Surry, S. L. Buchwald, *Org. Lett.* **2013**, *15*, 3734 – 3737; c) A. Borzenko, N. L. Rotta-Loria, P. M. MacQueen, C. M. Lavoie, R. McDonald, M. Stradiotto, *Angew. Chem. Int. Ed.* **2015**, *54*, 3773 – 3777; *Angew. Chem.* **2015**, *127*, 3844 – 3848; d) M. Zhu, K.-i. Fujita, R. Yamaguchi, *Org. Lett.* **2010**, *12*, 1336 – 1339; e) F. Shi, M. K. Tse, X. Cui, D. Gordes, D. Michalik, K. Thurow, Y. Deng, M. Beller, *Angew. Chem. Int. Ed.* **2009**, *48*, 5912 – 5915; *Angew. Chem.* **2009**, *121*, 6026 – 6029; f) M. H. S. A. Hamid, C. L. Allen, G. W. Lamb, A. C. Maxwell, H. C. Maytum, A. J. A. Watson, J. M. J. Williams, *J. Am. Chem. Soc.* **2009**, *131*, 1766 – 1774.

[24] C. U. Grünanger, B. Breit, *Angew. Chem. Int. Ed.* **2008**, *47*, 7346 – 7349; *Angew. Chem.* **2008**, *120*, 7456 – 7459.

[25] a) M. Montag, J. Zhang, D. Milstein, *J. Am. Chem. Soc.* **2012**, *134*, 10325 – 10328; b) C. A. Huff, J. W. Kampf, M. S. Sanford, *Organometallics* **2012**, *31*, 4643 – 4645; d) C. A. Huff, J. W. Kampf, M. S. Sanford, *Chem. Commun.* **2013**, *49*, 7147 – 7149.

[26] Bruker, *APEX2 software*, Madison, WI, USA, 2014.

[27] G. M. Sheldrick, *SADABS: Area-Detector Absorption Correction*, Universität Göttingen, Germany, **1999**.

[28] G. M. Sheldrick, *Acta Crystallogr. Sect. A* **2008**, *64*, 112.

[29] A. L. Spek, *Acta Crystallogr. Sect. D* **2009**, *65*, 148.

[30] R. Ahlrichs, Turbomole Version 6.5, Theoretical Chemistry Group, University of Karlsruhe.

[31] PQS version 2.4, **2001**, Parallel Quantum Solutions, Fayettevile, Arkansas (USA); the Baker optimizer is available separately from PQS upon request: I. Baker, *J. Comput. Chem.* **1986**, *7*, 385.

[32] P. H. M. Budzelaar, *J. Comput. Chem.* **2007**, *28*, 2226.

[33] M. Sierka, A. Hogekamp, R. Ahlrichs, *J. Chem. Phys.* **2003**, *118*, 9136.

[34] a) A. D. Becke, *Phys. Rev. A* **1988**, *38*, 3098; b) J. P. Perdew, *Phys. Rev. B* **1986**, *33*, 8822.

[35] a) F. Weigend, R. Ahlrichs, *Phys. Chem. Chem. Phys.* **2005**, *7*, 3297; b) F. Weigend, M. Häser, H. Patzelt, R. Ahlrichs, *Chem. Phys. Lett.* **1998**, *294*, 143.

[36] W. Humphrey, A. Dalke, K. Schulten, *J. Mol. Graph.* **1996**, *14*, 33.

Received: April 14, 2015
Published online on July 17, 2015